This article has been accepted for inclusion in a future issue of this journal. Content is final as presented, with the exception of pagination.

Observer-Based Event-Triggered Control for Networked Linear Systems Subject to Denial-of-Service Attacks

Songlin Hu, Dong Yue, *Senior Member, IEEE*, Qing-Long Han, *Fellow, IEEE*, Xiangpeng Xie, Xiaoli Chen, and Chunxia Dou

***Abstract*—This paper is concerned with the observer-based event-triggered control for a continuous networked linear system subject to denial-of-service (DoS) attacks, where the attacks are launched periodically to block the data transmission in control channels. First, a new observer state-based resilient event-triggering scheme is developed in the presence of DoS attacks. Second, a novel event-based switched system model is established by considering the effect of the event-triggering scheme and DoS attacks simultaneously. By virtue of this new model combined with a piecewise Lyapunov–Krasovskii functional method, the sufficient conditions are derived to guarantee exponential stability of the resulting switched system. It is shown that the proposed results can establish a quantitative relationship among the launching/sleeping periods of the attacks, the event-triggering parameters, the sampling period, and the exponential decay rate. Third, criteria for designing a desired observer-based event-triggered controller are provided and expressed in terms of a set of linear matrix inequalities. Finally, an offshore structure model is presented to illustrate the efficiency of the developed control method.**

***Index Terms*—Cyber-physical systems (CPSs), denial-of-service (DoS) attacks, networked control systems (NCSs), piecewise Lyapunov–Krasovskii functional, resilient event-triggered communication scheme.**

I. Introduction

RECENT advances in hardware, sensing, and communication technologies have enabled the rapid development of cyber-physical systems (CPSs), which integrate computation, communication networks, and physical plants. CPSs have been used in many areas, such as aerospace, automotive, chemical processes, healthcare, manufacturing, critical infrastructures [1], to name a few. However, although CPSs have many benefits, they also pose several challenges. One of the most challenging issues in CPSs is cyber security at the cyber layer, as communication links (especially wireless communication link) are vulnerable to malicious attacks. Recently, considerable research attention of secure monitoring and control for CPSs has gained attention [2]–[4]. As commented in [5], the main security concerns in CPSs, particularly in networked control systems (NCSs), lie in two types of attacks: 1) deception attacks and 2) denial-of-service (DoS) attacks. The former aims to alter the integrity of transmitted data [6], [7], while the latter, launched by external jammers, attempts to compromise the availability of transmitted data at their destinations [8]. We refer to the recent survey [9] for more information on these attacks.

In a practical control system, especially monitored over a wireless communication network, network components, such as sensors and controllers may have restricted sensing, processing, and computational capabilities. The bandwidth of the wireless network may also be finite in certain scenarios such as low bit rates within an underwater communication environment [10]. To reduce frequent occupancy of these computation and network resources, many different event-triggered schemes have been put forward (see [11]–[14] for a single continuous-time system and [15], [16] for multiagent systems), which makes the event-triggered control (ETC) a promising solution for NCSs subject to constrained resources. Generally, an ETC scheme is such a control strategy that can improve the efficiency of using computation and network resources while preserving the satisfactory closed-loop system performance. Until now, several methods on designing ETC schemes for NCSs have been reported in [11]–[14] and [17]–[26].

Note that most existing results aforementioned do not take cyber-security issues into account with a few exceptions [27]–[34]. For example, in [27], the stability problem of a networked linear continuous-time system under power-constraint, known and unknown, pulse-width modulated DoS attack signals is addressed. In [28], a more general DoS attack model is proposed where the feature of DoS attacks is characterized by DoS frequency and DoS duration. Based on a

Manuscript received October 13, 2018; revised January 5, 2019; accepted February 28, 2019. This work was supported in part by the National Natural Science Foundation of China under Grant 61673223, Grant 61833008, and Grant 61773221, in part by the "Six Talent Peaks Project" of Jiangsu Province of China under Grant RLD201810, in part by the QingLan Project of Jiangsu Province of China under Grant QL 04317006, in part by NUPTSF under Grant XJKY15001, and in part by the Australian Research Council Discovery Project under Grant DP160103567. This paper was recommended by Associate Editor C. Hua. *(Corresponding authors: Dong Yue; Qing-Long Han.)*

S. Hu, D. Yue, X. Xie, and C. Dou are with the Institute of Advanced Technology, Nanjing University of Posts and Telecommunications, Nanjing 210023, China (e-mail: songlin621@126.com; medongy@vip.163.com; xiexiangpeng1953@163.com; cxdou@ysu.edu.cn).

Q.-L. Han is with the School of Software and Electrical Engineering, Swinburne University of Technology, Melbourne, VIC 3122, Australia (e-mail: qhan@swin.edu.au).

X. Chen is with the School of Telecommunications and Information, Engineering, Nanjing University of Posts and Telecommunications, Nanjing 210003, China (e-mail: chenxiaoli206@126.com).

Color versions of one or more of the figures in this paper are available online at http://ieeexplore.ieee.org.

Digital Object Identifier 10.1109/TCYB.2019.2903817

similar idea, extensions have been considered in [5] and [30] for dealing with dynamic output-feedback controllers, in [33] for nonlinear NCSs, and in [35] for distributed NCSs. In [29], the stability and stabilization problems of a networked linear discrete-time system with random packet losses and malicious attacks is investigated. In [31], a zero-sum static game framework is applied to deal with the optimal control and scheduling problem for a linear NCS with communication constraints and DoS attacks. In [32], a resilient event-triggering H_∞ load frequency control synthesis method is developed for a networked multiarea power system under energy-limited random DoS attacks, where DoS duration is assumed to be within a finite interval. Nevertheless, it should be pointed out that most of the results above-mentioned are limited to performance analysis, while leaving controller synthesis unexplored. Moreover, these results assume the availability of full system state information so that state-feedback control laws can be designed, which limits their application in practical control systems as it is common that only partial observation of a practical system state is measurable due to limited communication and/or computation resources or the presence of unavoidable noise [36]. Based on the observations above, the following question naturally arises: Is it possible to develop a unified observer-based output-feedback scheme which not only preserves desirable system performance (stability) and meets resource-efficient requirement but also satisfies satisfactory resilience requirement exposed by malicious attacks? How to well solve this problem such that the simultaneous effects of malicious attacks, limited computation, and network resources, and unavailable full state information can be handled in a unified manner motivates this paper.

In this paper, we will address an issue about observer-based control design for a continuous linear NCS under limited resources and DoS attacks. The system will be remotely controlled and observed via a wireless network. The main contributions are summarized as follows.

1) *A new event triggering mechanism* based on the observer state will be proposed. It will be shown that a positive minimum interevent time always exists so that Zeno behavior can be excluded naturally.
2) A quantitative relation among the exponential convergence rate, the sampling period, the "active" and "sleeping" periods of DoS attacks is explicitly characterized.
3) *A novel observer-based resilient ETC strategy* will be developed to ensure that the resultant switched system is globally exponentially stable (GES) and resilient to DoS attacks as well. The main stability analysis and control design results will be formulated and expressed by resorting to LMIs and will be numerically efficient to verify.

This paper is organized as follows. In Section II, a unified event-triggered NCS model under the periodic DoS attacks is proposed. In Section III, exponential stability of the closed-loop system is analyzed. Furthermore, triggering matrix, controller gain matrix, and observer gain matrices are obtained by solving a set of LMIs. In Section IV, the effectiveness of the proposed control strategy is demonstrated by a practical example. The conclusions are drawn in Section V.

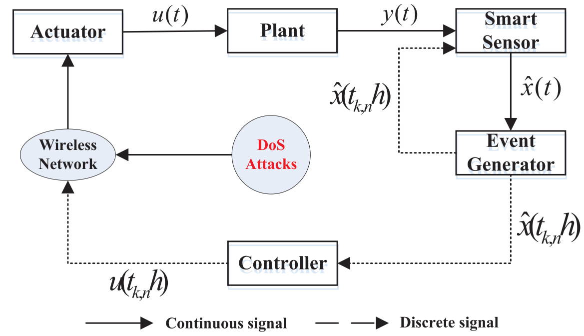

Fig. 1. Block diagram of an event-triggered NCS under DoS attacks.

II. Preliminaries and Problem Formulation

As shown in Fig. 1, the NCS configuration under consideration consists of a physical plant, a smart sensor, an event generator, a controller, and an actuator. The signal transmission from sensor to controller, and controller to actuator is implemented via a digital channel, which can be compromised by certain DoS jamming signals. In the following, we will describe each component in detail.

A. Physical Plant

The dynamics of the physical plant shown in Fig. 1 is given by

$$\begin{cases} \dot{x}(t) = Ax(t) + Bu(t) \\ y(t) = Cx(t) \\ x(0) = x_0 \end{cases} \tag{1}$$

where $x(t) \in \mathbb{R}^{n_x}$ is the state vector, $u(t) \in \mathbb{R}^m$ is the control input, $y(t) \in \mathbb{R}^q$ is the output vector, and n_x, m, and $q \in \mathbb{N}$, $\mathbb{N}$ represents the set of non-negative integers. A, B, and C are the constant matrices of appropriate dimensions. x_0 is the initial condition. Throughout this paper, it is assumed that: 1) the state vector $x(t)$ is unmeasurable; 2) the pairs (A, B) and (A, C) are controllable and observable, respectively; and 3) the matrix C is of full row rank.

B. DoS Jamming Attacks

Following [27], we consider a type of power-constraint, periodic jammer signal, and blocking the digital communication channel as follows:

$$\mathcal{I}_{\text{DoS}}(t) = \begin{cases} 0, & t \in \left[nT, nT + T_{\text{off}}^{\min}\right) \\ 1, & t \in \left[nT + T_{\text{off}}^{\min}, (n+1)T\right) \end{cases} \tag{2}$$

where $n \in \mathbb{N}$ is the period number, $T > 0$ is the action period of the jammer, and $T_{\text{off}}^{\min}$ $(0 < T_{\text{off}}^{\min} < T)$ denotes the sleeping period of the jammer in the nth period. Moreover, the sets $\cup_{n\in\mathbb{N}}[nT, nT + T_{\text{off}}^{\min})$ denote the intervals over which the jamming signal is off and communication is allowed, while the sets $\cup_{n\in\mathbb{N}}[nT+T_{\text{off}}^{\min}, (n+1)T)$ denote the intervals over which the jamming signal is active and communication is denied, and thus no data can be transmitted in these time intervals. In the following, for notational simplicity, let $\mathcal{L}_{1,n} \triangleq [nT, nT+T_{\text{off}}^{\min})$, $\mathcal{L}_{2,n} \triangleq [nT+T_{\text{off}}^{\min}, (n+1)T)$.

Remark 1: It should be pointed out that the parameter $T_{\text{off}}^{\min}$ in (2) needs not to be time-invariant, and thus we assume that there exists a uniform lower bound for the sleeping period $T_{\text{off}}^{\min}$ as in [27]. Throughout this paper, for simplicity, we use the parameter $T_{\text{off}}^{\min}$ to denote the uniform lower bound of the sleeping period in every active period T.

C. Smart Sensor

The smart sensor has great computational power and can preprocess measurement output $y(t)$ to get the state estimate $\hat{x}(t)$ based on the following switched full-order state observer despite the presence of the DoS jamming attacks (2):

$$\begin{cases} \dot{\hat{x}}(t) = \begin{cases} A\hat{x}(t) + Bu(t) + L_1\big[y(t) - \hat{y}(t)\big] \\ t \in \mathcal{L}_{1,n}, n \in \mathbb{N} \\ A\hat{x}(t) + Bu(t) + L_2\big[y(t) - \hat{y}(t)\big] \\ t \in \mathcal{L}_{2,n}, n \in \mathbb{N} \end{cases} \\ \hat{y}(t) = C\hat{x}(t), \hat{x}(0) = \hat{x}_0 \end{cases} \tag{3}$$

where $\hat{x}(t) \in \mathbb{R}^n$ is the observer state, $\hat{y}(t) \in \mathbb{R}^q$ is the observer output, L_1 and $L_2 \in \mathbb{R}^{n\times q}$ are the observer gains to be designed later, and $\hat{x}_0$ is the initial condition of the observer.

Remark 2: Note that in (3), two different observer gain matrices are introduced corresponding to the "sleeping mode" and "activated state" of the DoS jamming attacks (2), respectively. By doing so, the observer can adapt the duty cycle of DoS jamming attacks. Moreover, it can be inferred that as $T_{\text{off}}^{\min} \to T$, the switched state observer (3) reduces to the traditional Luenberger observer $\dot{\hat{x}}(t) = A\hat{x}(t) + Bu(t) + L_1[y(t) - \hat{y}(t)]$. Therefore, the traditional Luenberger observer can be regarded as a special case of the observer (3).

D. Resilient Triggering Condition and Observer-Based ETC Structure

In this paper, inspired by sampled-data-based event-triggered schemes [24], [25], and PETC schemes [26], we will propose a resilient triggering scheme. In doing so, we select the condition

$$e_{k_j}^T\big(t_{k_j}h\big)\Omega e_{k_j}\big(t_{k_j}h\big) > \varepsilon\hat{x}^T(t_kh)\Omega\hat{x}(t_kh) \tag{4}$$

where $e_{k_j}(t_{k_j}h) = \hat{x}(t_{k_j}h) - \hat{x}(t_kh)$, $\varepsilon \in (0, 1)$ is a design parameter, $t_{k_j}h \triangleq t_kh + jh$ denotes the sampling instant between two consecutive triggering instant, t_kh is the latest event-triggering instant, and Ω is a positive definite weighting matrix to be designed later.

Then in the presence of the periodic DoS jamming attacks (2), the triggering instant when the event generator transmits the estimate $\hat{x}(t)$ to the controller is determined by the following resilient triggering condition described by:

$$t_{k,n}h = \big\{t_{k_j}h \text{ satisfying (4)} | t_{k_j}h \in \bar{\mathcal{L}}_{1,n}\big\} \cup \{nT\} \tag{5}$$

where n, k_j, $j \in \mathbb{N}$, and k is the number of triggering times occurring in the nth jammer action period. The parameter $h > 0$ denotes the sampling period. $t_{1,n}h \overset{\triangle}{=} (n-1)T$, $0 < h < T$, $\bar{\mathcal{L}}_{1,n} \triangleq [(n-1)T, (n-1)T + T_{\text{off}}^{\min})$, $\bar{\mathcal{L}}_{2,n} \triangleq [(n-1)T + T_{\text{off}}^{\min}, nT)$.

In what follows, inspired by [37, Remark 1], under the DoS jamming attacks, the observer-based ETC $u(t)$ can be written as

$$u(t) = \begin{cases} K\hat{x}\big(t_{k,n}h\big), & t \in \big[t_{k,n}h, t_{k+1,n}h\big) \cap \bar{\mathcal{L}}_{1,n} \\ 0, & t \in \bar{\mathcal{L}}_{2,n}, n \in \mathbb{N} \end{cases} \tag{6}$$

where K is the control gain matrix, the sequence $\{t_{k,n}h\}$ can be iteratively determined by the above event-triggering condition (5), $k \in \{1, \ldots, k(n)\} \overset{\triangle}{=} K(n)$ with

$$k(n) = \sup\Big\{k \in \mathbb{N} | t_{k,n}h \le (n-1)T + T_{\text{off}}^{\min}\Big\}$$

which implies that $t_{k(n)+1,n}h > (n-1)T + T_{\text{off}}^{\min}$.

Remark 3: Notice that the zero-input strategy is employed when the DoS attacks are active. In doing so, the actuator does not work during the jamming period, which in turn reduces the energy consumption at the actuator side. In fact, the zero-input strategy has been widely used in [38]–[40]. However, these results do not consider the effects of the DoS attacks. In particular, when $T_{\text{off}}^{\min} \to T$, it implies that the jamming signal has all but disappeared and the communication can be maintained continuously. This case has been extensively studied in the context of an ETC framework (see [25] and the references therein).

E. Modeling of the Observer-Based ETC Systems Under DoS Attacks

In the sequel, for simplicity of exposition, for $n \in \mathbb{N}$, define $\Upsilon_{k,n} \overset{\triangle}{=} [t_{k,n}h, t_{k+1,n}h)$, $k \in K(n)$. Substituting (6) into (1) yields

$$\dot{x}(t) = \begin{cases} Ax(t) + BK\hat{x}\big(t_{k,n}h\big), & t \in \Upsilon_{k,n} \cap \bar{\mathcal{L}}_{1,n} \\ Ax(t), & t \in \bar{\mathcal{L}}_{2,n}. \end{cases} \tag{7}$$

For technical analysis, we divide the event intervals $\Upsilon_{k,n}$ shown in (7) into sampling interval-like subintervals, that is

$$\Upsilon_{k,n} = \cup_{l=1}^{\gamma_{k,n}}\big[t_{k,n}h + (l-1)h, t_{k,n}h + lh\big) \tag{8}$$

where $k \in K(n)$, $n \in \mathbb{N}$, and $\gamma_{k,n} \overset{\triangle}{=} \inf\{l \in \mathbb{N} | t_{k,n}h + lh \ge t_{k+1,n}h\}$.

Let

$$\begin{cases} \mathcal{F}_{k,n}^l = \big[t_{k,n}h + (l-1)h, t_{k,n}h + lh\big) \\ l \in \big\{1, 2, \ldots, \gamma_{k,n} - 1\big\} \\ \mathcal{F}_{k,n}^{\gamma_{k,n}} = \big[t_{k,n}h + \big(\gamma_{k,n} - 1\big)h, t_{k+1,n}h\big). \end{cases} \tag{9}$$

Note that

$$\bar{\mathcal{L}}_{1,n} = \cup_{k=1}^{k(n)}\big\{\Upsilon_{k,n} \cap \bar{\mathcal{L}}_{1,n}\big\} \subseteq \cup_{k=1}^{k(n)}\Upsilon_{k,n}. \tag{10}$$

Combining (8)–(10), the interval $\bar{\mathcal{L}}_{1,n}$ can be rewritten as

$$\bar{\mathcal{L}}_{1,n} = \cup_{k=1}^{k(n)} \cup_{l=1}^{\gamma_{k,n}} \Big\{\mathcal{F}_{k,n}^l \cap \bar{\mathcal{L}}_{1,n}\Big\}.$$

Set

$$\Psi_{k,n}^{l}=\mathcal{F}_{k,n}^{l}\cap\bar{\mathcal{L}}_{1,n}.$$

Then

$$\bar{\mathcal{L}}_{1,n}=\cup_{k=1}^{k(n)}\cup_{l=1}^{\gamma_{k,n}}\Psi_{k,n}^{l}.$$

Now, for $k\in K(n)$, $n\in\mathbb{N}$, we define two piecewise functions as follows:

$$\tau_{k,n}(t)=\begin{cases}t-t_{k,n}h,\ t\in\Psi_{k,n}^{1}\\ t-t_{k,n}h-h,\ t\in\Psi_{k,n}^{2}\\ \vdots\\ t-t_{k,n}h-\big(\gamma_{k,n}-1\big)h,\ t\in\Psi_{k,n}^{\gamma_{k,n}}\end{cases}\tag{11}$$

and

$$e_{k,n}(t)=\begin{cases}0,\quad t\in\Psi_{k,n}^{1}\\ \hat{x}\big(t_{k,n}h\big)-\hat{x}\big(t_{k,n}h+h\big),\quad t\in\Psi_{k,n}^{2}\\ \vdots\\ \hat{x}\big(t_{k,n}h\big)-\hat{x}\big(t_{k,n}h+\big(\gamma_{k,n}-1\big)h\big)\\ t\in\Psi_{k,n}^{\gamma_{k,n}}.\end{cases}\tag{12}$$

Based on the above two definitions, it can be seen that

$$\hat{x}\big(t_{k,n}h\big)=\hat{x}\big(t-\tau_{k,n}(t)\big)+e_{k,n}(t)\tag{13}$$

where $\tau_{k,n}(t)\in[0,h)$, $t\in\Upsilon_{k,n}\cap\bar{\mathcal{L}}_{1,n}$, $k\in K(n)$.

Then, the system (7) can be described as

$$\begin{cases}\dot{x}(t)=\begin{cases}Ax(t)+BK\hat{x}\big(t-\tau_{k,n}(t)\big)\\ \quad+BKe_{k,n}(t),\quad t\in\Upsilon_{k,n}\cap\bar{\mathcal{L}}_{1,n}\\ Ax(t),\ t\in\bar{\mathcal{L}}_{2,n}\end{cases}\\ x(t)=\phi_1(t),\ t\in[-h,0]\end{cases}\tag{14}$$

where $\phi_1(t)$ is the supplemented initial condition of the state $x(t)$ on $[-h,0]$, and the error vector $e_{k,n}(t)$ satisfies

$$\begin{aligned}e_{k,n}^{T}(t)\Omega e_{k,n}(t)\le{}&\varepsilon\big[\hat{x}\big(t-\tau_{k,n}(t)\big)+e_{k,n}(t)\big]^{T}\\ &\Omega\big[\hat{x}\big(t-\tau_{k,n}(t)\big)+e_{k,n}(t)\big].\end{aligned}\tag{15}$$

Substituting (6) and (13) into system (3), the observer system under the DoS attack can be rewritten as

$$\begin{cases}\dot{\hat{x}}(t)=\begin{cases}A\hat{x}(t)+BK\hat{x}\big(t-\tau_{k,n}(t)\big)+BKe_{k,n}(t)\\ \quad+L_1C\big[x(t)-\hat{x}(t)\big],\ t\in\Upsilon_{k,n}\cap\bar{\mathcal{L}}_{1,n}\\ A\hat{x}(t)+L_2C\big[x(t)-\hat{x}(t)\big],\ t\in\bar{\mathcal{L}}_{2,n}\end{cases}\\ \hat{x}(t)=\phi_2(t),\ t\in[-h,0]\end{cases}\tag{16}$$

where $\phi_2(t)$ is the supplemented initial condition of the state $\hat{x}(t)$ on $[-h,0]$. Define $\tilde{x}(t)=x(t)-\hat{x}(t)$, then

$$\dot{\tilde{x}}(t)=\begin{cases}(A-L_1C)\tilde{x}(t),\ \ t\in\Upsilon_{k,n}\cap\bar{\mathcal{L}}_{1,n}\\ (A-L_2C)\tilde{x}(t),\ \ t\in\bar{\mathcal{L}}_{2,n}.\end{cases}\tag{17}$$

Define $\xi^{T}(t)=[\hat{x}^{T}(t),\tilde{x}^{T}(t)]$. We have the following switched system:

$$\begin{cases}\dot{\xi}(t)=\begin{cases}A_1\xi(t)+B_1G\xi\big(t-\tau_{k,n}(t)\big)\\ \quad+B_1e_{k,n}(t),\ \ t\in\Upsilon_{k,n}\cap\bar{\mathcal{L}}_{1,n},k\in K(n)\\ A_2\xi(t),\ \ t\in\bar{\mathcal{L}}_{2,n},n\in\mathbb{N}\end{cases}\\ \xi(t)=\phi(t),\ \ t\in[-h,0]\end{cases}\tag{18}$$

where

$$\begin{aligned}&A_1=\begin{bmatrix}A & L_1C\\ 0 & A-L_1C\end{bmatrix},\ B_1=\begin{bmatrix}BK\\ 0\end{bmatrix}\\ &A_2=\begin{bmatrix}A & L_2C\\ 0 & A-L_2C\end{bmatrix},\ \phi(t)=\phi_t=\begin{bmatrix}\phi_1(t)\\ \phi_1(t)-\phi_2(t)\end{bmatrix}\\ &G=\begin{bmatrix}I & 0\end{bmatrix}.\end{aligned}$$

F. Problem Formulation

Throughout this paper, we shall use the following definition of global exponential stability for the switched system (18).

Definition 1: The switched system (18) is said to be GES, if there exists a scalar $\kappa>0$ such that the solution $\xi(t)$ of the system (18) satisfies $\|\xi(t)\|\le\kappa e^{-\rho t}\|\phi_0\|_h$, $t\ge 0$, where $\|\phi_t\|_h\triangleq\sup_{-h\le\theta\le 0}\{\|x(t+\theta)\|,\|\dot{x}(t+\theta)\|\}$ and ρ is called the decay rate.

The control objective of this paper is to jointly design the observer and event-triggering scheme such that, for all possible periodic jamming attacks $\mathcal{I}_{\mathrm{DoS}}(t)$ (2), where the sequence $\{nT\}_{n\in\mathbb{N}}$ and parameters T and $T_{\mathrm{off}}^{\min}$ are known ($T_{\mathrm{off}}^{\min}\le T<+\infty$), the switched system (18) is GES.

III. Main Results

The following lemma estimates the upper bounds of the chosen Lyapunov functional candidate in the absence of DoS attacks and in the presence of DoS attacks, respectively. Note that these estimations will later be used to characterize the properties of DoS attacks that guarantee the GES of the resultant switched system (18).

Lemma 1: Given the feedback gain K and a jamming signal $\mathcal{I}_{\mathrm{DoS}}(t)$ (2), where the sequence $\{nT\}_{n\in\mathbb{N}}$ and parameters T and $T_{\mathrm{off}}^{\min}$ are known ($T_{\mathrm{off}}^{\min}\le T<+\infty$). For the system (18), if for some prescribed constants $\alpha_i\in(0,+\infty)$, $\varepsilon\in(0,1)$, and $h\in(0,T_{\mathrm{off}}^{\min})$, there exist symmetric positive definite matrices P_i, Q_i, and R_i, and matrices U_i $(i=1,2)$ of appropriate dimensions such that

$$\Pi_1<0,\Re_1>0\tag{19}$$

$$\Pi_2<0,\Re_2>0\tag{20}$$

where

$$\begin{aligned}&\Pi_1=\begin{bmatrix}\Sigma_1 & *\\ hR_1GF_1 & -R_1\end{bmatrix},\Re_1=\begin{bmatrix}\tilde{R}_1 & *\\ U_1 & \tilde{R}_1\end{bmatrix}\\ &\Pi_2=\begin{bmatrix}\Sigma_2 & *\\ hR_2GF_2 & -R_2\end{bmatrix},\Re_2=\begin{bmatrix}\tilde{R}_2 & *\\ U_2 & \tilde{R}_2\end{bmatrix}\\ &\tilde{R}_1=e^{-2\alpha_1 h}\begin{bmatrix}R_1 & *\\ 0 & 3R_1\end{bmatrix},U_1=\begin{bmatrix}U_{11} & U_{12}\\ U_{13} & U_{14}\end{bmatrix}\\ &\tilde{R}_2=\begin{bmatrix}R_2 & *\\ 0 & 3R_2\end{bmatrix},U_2=\begin{bmatrix}U_{21} & U_{22}\\ U_{23} & U_{24}\end{bmatrix}\\ &\Sigma_1=\begin{bmatrix}\Sigma_1^{11} & * & * & * & * & *\\ \Sigma_1^{21} & \Sigma_1^{22} & * & * & * & *\\ \Sigma_1^{31} & \Sigma_1^{32} & \Sigma_1^{33} & * & * & *\\ \Sigma_1^{41} & \Sigma_1^{42} & \Sigma_1^{43} & \Sigma_1^{44} & * & *\\ \Sigma_1^{51} & \Sigma_1^{52} & \Sigma_1^{53} & \Sigma_1^{54} & \Sigma_1^{55} & *\\ \Sigma_1^{61} & \Sigma_1^{62} & 0 & 0 & 0 & \Sigma_1^{66}\end{bmatrix}\end{aligned}$$

$$\Sigma_2 = \begin{bmatrix} \Sigma_2^{11} & * & * & * & * \\ \Sigma_2^{21} & \Sigma_2^{22} & * & * & * \\ \Sigma_2^{31} & \Sigma_2^{32} & \Sigma_2^{33} & * & * \\ \Sigma_2^{41} & \Sigma_2^{42} & \Sigma_2^{43} & \Sigma_2^{44} & * \\ \Sigma_2^{51} & \Sigma_2^{52} & \Sigma_2^{53} & \Sigma_2^{54} & \Sigma_2^{55} \end{bmatrix}$$

$$\begin{aligned}
\Sigma_1^{11} &= 2\alpha_1 P_1 + \mathrm{He}(P_1 A_1) \\
&\quad + G^T Q_1 G - 4e^{-2\alpha_1 h} G^T R_1 G \\
\Sigma_1^{21} &= B_1^T P_1 - 2e^{-2\alpha_1 h} R_1 G - U_{11} G \\
&\quad - U_{12} G - U_{13} G - U_{14} G \\
\Sigma_1^{22} &= \varepsilon\Omega - 8e^{-2\alpha_1 h} R_1 + \mathrm{He}(U_{11} - U_{12}) \\
&\quad + \mathrm{He}(U_{13} - U_{14}) \\
\Sigma_1^{31} &= U_{11} G + U_{12} G - U_{13} G - U_{14} G \\
\Sigma_1^{32} &= -2e^{-2\alpha_1 h} R_1 - U_{11} + U_{12} + U_{13} - U_{14} \\
\Sigma_1^{33} &= -e^{-2\alpha_1 h} Q_1 - 4e^{-2\alpha_1 h} R_1,\ \Sigma_1^{41} = 6e^{-2\alpha_1 h} R_1 G \\
\Sigma_1^{42} &= 6e^{-2\alpha_1 h} R_1 + 2U_{12}^T + 2U_{14}^T \\
\Sigma_1^{43} &= -2U_{12}^T + 2U_{14}^T,\ \Sigma_1^{44} = -12e^{-2\alpha_1 h} R_1 \\
\Sigma_1^{51} &= 2U_{13} G + 2U_{14} G,\ \Sigma_1^{53} = 6e^{-2\alpha_1 h} R_1 \\
\Sigma_1^{52} &= 6e^{-2\alpha_1 h} R_1 - 2U_{13} + 2U_{14} \\
\Sigma_1^{54} &= -4U_{14},\ \Sigma_1^{55} = -12e^{-2\alpha_1 h} R_1 \\
\Sigma_1^{61} &= B_1^T P_1,\ \Sigma_1^{62} = \varepsilon\Omega,\ \Sigma_1^{66} = (\varepsilon - 1)\Omega \\
F_1 &= \begin{bmatrix} A_1 & B_1 & 0 & 0 & 0 & B_1 \end{bmatrix} \\
\Sigma_2^{11} &= -2\alpha_2 P_2 + \mathrm{He}(P_2 A_2) + G^T Q_2 G - 4G^T R_2 G \\
\Sigma_2^{21} &= -2R_2 G - U_{21} G - U_{22} G - U_{23} G - U_{24} G \\
\Sigma_2^{22} &= -8R_2 + \mathrm{He}(U_{21} - U_{22} + U_{23} - U_{24}) \\
\Sigma_2^{31} &= U_{21} G + U_{22} G - U_{23} G - U_{24} G \\
\Sigma_2^{32} &= -2R_2 - U_{21} + U_{22} + U_{23} - U_{24} \\
\Sigma_2^{33} &= -e^{2\alpha_2 h} Q_2 - 4R_2,\ \Sigma_2^{41} = 6R_2 G \\
\Sigma_2^{42} &= 6R_2 + 2U_{22}^T + 2U_{24}^T,\ \Sigma_2^{44} = -12R_2 \\
\Sigma_2^{43} &= -2U_{22}^T + 2U_{24}^T,\ \Sigma_2^{53} = 6R_2,\ \Sigma_2^{54} = -4U_{24} \\
\Sigma_2^{51} &= 2U_{23} G + 2U_{24} G,\ \Sigma_2^{52} = 6R_2 - 2(U_{23} - U_{24}) \\
\Sigma_2^{55} &= -12R_2,\ F_2 = \begin{bmatrix} A_2 & 0 & 0 & 0 & 0 \end{bmatrix}.
\end{aligned}$$

Then along the trajectory of the system (18), it follows that:

$$V(t) \le \begin{cases} \rho_1(nT)V(nT), & t \in \bar{\mathcal{L}}_{1,n} \\ \rho_2\big(nT + T_{\text{off}}^{\min}\big)V\big(nT + T_{\text{off}}^{\min}\big), & t \in \bar{\mathcal{L}}_{2,n} \end{cases} \tag{21}$$

where $\rho_1(s) = e^{-2\alpha_1(t-s)}$ and $\rho_2(s) = e^{2\alpha_2(t-s)}$.

Proof: See Appendix A. ■

Based on Lemma 1, we now state and establish the following stability analysis result.

Theorem 1: Given the feedback gain K and a jamming signal $\mathcal{I}_{\text{DoS}}(t)$ (2), and the sequence $\{nT\}_{n\in\mathbb{N}}$ and parameters T and $T_{\text{off}}^{\min}$ are known ($T_{\text{off}}^{\min} \le T < +\infty$). For the system (18), if for some prescribed constants $\alpha_i \in (0, +\infty)$, $\mu_i \in (0, +\infty)$ ($i = 1, 2$, $\mu_1\mu_2 \ge 1$), $\varepsilon \in (0, 1)$, $h \in (0, T_{\text{off}}^{\min})$ satisfying

$$T_{\text{off}}^{\min} > \frac{2\alpha_2 T + 2(\alpha_1 + \alpha_2)h + \ln(\mu_1\mu_2)}{2(\alpha_1 + \alpha_2)} \tag{22}$$

there exist symmetric positive definite matrices $P_i \in \mathbb{R}^{2n\times 2n}$, $Q_i \in \mathbb{R}^{n\times n}$, $R_i \in \mathbb{R}^{n\times n}$, and $\Omega \in \mathbb{R}^{n\times n}$ and matrices U_i ($i = 1, 2$) of appropriate dimensions such that the LMIs (19) and (20) and the conditions below are satisfied

$$P_1 \le \mu_2 P_2 \tag{23}$$
$$e^{-2(\alpha_1+\alpha_2)h} P_2 \le \mu_1 P_1 \tag{24}$$
$$Q_1 \le \mu_2 Q_2 \tag{25}$$
$$R_1 \le \mu_2 R_2 \tag{26}$$
$$Q_2 \le \mu_1 Q_1 \tag{27}$$
$$R_2 \le \mu_1 R_1 \tag{28}$$

then the switched system (18) under the periodic DoS jamming attacks (2) is GES with the decay rate $\rho \triangleq (\lambda/2T)$, $\lambda \triangleq 2\alpha_1 T_{\text{off}}^{\min} - 2\alpha_2(T - T_{\text{off}}^{\min}) - 2(\alpha_1 + \alpha_2)h - \ln(\mu_1\mu_2)$.

Proof: See Appendix B. ■

Remark 4: From (22), one can obtain the lower bound T_{off}^* of $T_{\text{off}}^{\min}$ as $T_{\text{off}}^* \triangleq [(2\alpha_2 T + 2(\alpha_1 + \alpha_2)h + \ln(\mu_1\mu_2))/(2(\alpha_1 + \alpha_2))]$, which depends on the jamming period T, the sampling period h, the convergence rate α_1 of the first subsystem of system (18), the divergence rate α_2 of the second subsystem of system (18), and two tuning parameters μ_i ($i = 1, 2$), simultaneously. When the parameters α_i, μ_i, and h are fixed, the larger the T, the larger the lower bound T_{off}^*, which is shown in Table I of Section IV (its numerical solution $T_{\text{off}}^{\min}$ is given by iteration, in theory, $T_{\text{off}}^* \le T_{\text{off}}^{\min}$). On the other hand, note that the decay rate $\rho \triangleq (\lambda/2T) = [(2\alpha_1 T_{\text{off}}^{\min} - 2\alpha_2(T - T_{\text{off}}^{\min}))/2T] - [(2(\alpha_1 + \alpha_2)h + \ln(\mu_1\mu_2))/2T] = [(2(\alpha_1 + \alpha_2)T_{\text{off}}^{\min})/2T] - [(2\alpha_2 T + 2(\alpha_1 + \alpha_2)h + \ln(\mu_1\mu_2))/2T] = [((\alpha_1+\alpha_2)(T_{\text{off}}^{\min} - T_{\text{off}}^*))/T]$. One can see that when the parameters α_i, μ_i ($i = 1, 2$), T, and h are fixed, the larger the $T_{\text{off}}^{\min}$, the larger the decay rate ρ, which is shown in Table II of Section IV.

Remark 5: Note that the inequalities (19), (20), and (23)–(28) are linear in P_i, Q_i, R_i, U_i, and Ω for fixed $\varepsilon \in (0, 1)$, K, $T \in (0, +\infty)$, $T_{\text{off}}^{\min} \in (0, T)$, $\alpha_i \in (0, +\infty)$, $\mu_i \in (0, +\infty)$ ($i = 1, 2$), and $h \in (0, T_{\text{off}}^{\min})$. Therefore, when the feedback gain matrix K and triggering parameter $\varepsilon \in (0, 1)$ are given in advance, feasible solutions P_i, Q_i, R_i, U_i, and Ω for LMIs (19), (20), and (23)–(28) can be searched by iterating over a set of values for $T \in (0, +\infty)$, $T_{\text{off}}^{\min} \in (0, T)$, $\alpha_i \in (0, +\infty)$, $\mu_i \in (0, +\infty)$, and $h \in (0, T_{\text{off}}^{\min})$ satisfying (22).

Remark 6: It should be pointed out that Theorem 1 provides a sufficient condition under which the system (18) is exponentially stable in the presence of the periodic DoS jamming attacks (2) if the maximum allowable jammer activity (MAJA) denoted by $J \triangleq [(T - T_{\text{off}}^{\min})/T] \times 100\%$ is smaller than a certain upper bound J^*. In fact, the inequality (22) is equivalent to $\lambda = 2\alpha_1 T_{\text{off}}^{\min} - 2\alpha_2(T - T_{\text{off}}^{\min}) - 2(\alpha_1 + \alpha_2)h - \ln(\mu_1\mu_2) > 0$. Also, note that the decay rate

$$\begin{aligned}
\rho &= \frac{\lambda}{2T} \\
&= \frac{2\alpha_1 T_{\text{off}}^{\min} - 2\alpha_2\big(T - T_{\text{off}}^{\min}\big)}{2T} \\
&\quad - \frac{2(\alpha_1 + \alpha_2)h + \ln(\mu_1\mu_2)}{2T} \\
&= \alpha_1(1 - J) - \alpha_2 J \\
&\quad - \frac{2(\alpha_1 + \alpha_2)h + \ln(\mu_1\mu_2)}{2T}.
\end{aligned} \tag{29}$$

Then due to the fact that $\lambda > 0 \Leftrightarrow \rho > 0$, one has

$$J < J^* \triangleq \frac{\alpha_1}{\alpha_1+\alpha_2} - \frac{2h(\alpha_1+\alpha_2)+\ln(\mu_1\mu_2)}{2T(\alpha_1+\alpha_2)}. \tag{30}$$

Remark 7: According to expressions (29) and (30), the following three conclusions can be drawn.

1) For given scalars $\alpha_i \in (0, +\infty)$, $\mu_i \in (0, +\infty)$ $(i = 1, 2)$, $T \in (0, +\infty)$, and $h \in (0, T)$, the exponential decay rate ρ is a linear monotonic decreasing function of the MAJA. That is, $\rho = \rho(J) = -(\alpha_1+\alpha_2)J + \alpha_1 - [(2(\alpha_1+\alpha_2)h + \ln(\mu_1\mu_2))/2T]$, which implies that the larger the J, the smaller the ρ, that is to say, the worse the stability performance.
2) For given scalars $\alpha_i \in (0, +\infty)$, $\mu_i \in (0, +\infty)$ $(i = 1, 2)$, $T \in (0, +\infty)$, and J, the exponential decay rate ρ is a linear monotonic decreasing function of the sampling period h. This relation can be explicitly expressed as $\rho = \rho(h) = -[((\alpha_1+\alpha_2))/T]h + \alpha_1 - [(\ln(\mu_1\mu_2))/2T] - (\alpha_1+\alpha_2)J$, from which one can see that a larger h results in a smaller ρ, and the vice-versa. So in order to improve the stability performance, one can reduce the sampling period value.
3) For given scalars $\alpha_i \in (0, +\infty)$, $\mu_i \in (0, +\infty)$ $(i = 1, 2)$, and $T \in (0, +\infty)$, the upper bound of the MAJA denoted by J^* is a linear monotonic decreasing function of the sampling period h, which is expressed as $J^* = J^*(h) = -(1/T)h + [\alpha_1/(\alpha_1+\alpha_2)] - [(\ln(\mu_1\mu_2))/(2T(\alpha_1+\alpha_2))]$, which implies that one can improve the tolerance of the ETC systems against the DoS jamming attacks by decreasing the sampling period.

By Theorem 1, we now provide the following theorem for the co-design of the observer gains L_1 and L_2, the controller gain K, and the weighting matrix Ω defining the resilient event-triggering scheme.

Theorem 2: Consider the jamming signal $\mathcal{I}_{\mathrm{DoS}}(t)$ (2), in which the sequence $\{nT\}_{n\in\mathbb{N}}$ and the parameters T and $T_{\mathrm{off}}^{\min}$ are known and $T_{\mathrm{off}}^{\min} \le T < +\infty$. For the system (18), if for given scalars $\alpha_i \in (0, +\infty)$, $\mu_i \in (0, +\infty)$, $\varepsilon \in (0, 1)$, and $h \in (0, T_{\mathrm{off}}^{\min})$ satisfying (22), $\varkappa_i$ and $\varpi_i \in (0, +\infty)$, there exist symmetric positive definite matrices $X_i \in \mathbb{R}^{2n\times 2n}$, $\bar{Q}_i \in \mathbb{R}^{n\times n}$, $\bar{R}_i \in \mathbb{R}^{n\times n}$, and $\bar{\Omega} \in \mathbb{R}^{n\times n}$, and matrices $\bar{U}_i$ $(i = 1, 2)$ of appropriate dimensions such that

$$\bar{\Pi}_1 < 0, \bar{\Re}_1 > 0 \tag{31}$$

$$\bar{\Pi}_2 < 0, \bar{\Re}_2 > 0 \tag{32}$$

$$\begin{bmatrix} -\mu_2 X_2 & * \\ X_2 & -X_1 \end{bmatrix} \le 0 \tag{33}$$

$$\begin{bmatrix} -\mu_1 e^{2(\alpha_1+\alpha_2)h} X_1 & * \\ X_1 & -X_2 \end{bmatrix} \le 0 \tag{34}$$

$$\begin{bmatrix} -\mu_2 \bar{Q}_2 & * \\ X_{21} & \varpi_1^2 \bar{Q}_1 - 2\varpi_1 X_{11} \end{bmatrix} \le 0 \tag{35}$$

$$\begin{bmatrix} -\mu_2 \bar{R}_2 & * \\ X_{21} & \varkappa_1^2 \bar{R}_1 - 2\varkappa_1 X_{11} \end{bmatrix} \le 0 \tag{36}$$

$$\begin{bmatrix} -\mu_1 \bar{Q}_1 & * \\ X_{11} & \varpi_2^2 \bar{Q}_2 - 2\varpi_2 X_{21} \end{bmatrix} \le 0 \tag{37}$$

$$\begin{bmatrix} -\mu_1 \bar{R}_1 & * \\ X_{11} & \varkappa_2^2 \bar{R}_2 - 2\varkappa_2 X_{21} \end{bmatrix} \le 0 \tag{38}$$

where

$$\bar{\Pi}_1 = \begin{bmatrix} \bar{\Sigma}_1 & * \\ h\bar{F}_1 & \varkappa_1^2 \bar{R}_1 - 2\varkappa_1 X_{11} \end{bmatrix}, \bar{\Re}_1 = \begin{bmatrix} \bar{\bar{R}}_1 & * \\ \bar{U}_1 & \bar{\bar{R}}_1 \end{bmatrix}$$

$$\bar{\Sigma}_1 = \begin{bmatrix} \bar{\Sigma}_1^{11} & * & * & * & * & * & * \\ \bar{\Sigma}_1^{21} & \bar{\Sigma}_1^{22} & * & * & * & * & * \\ \bar{\Sigma}_1^{31} & 0 & \bar{\Sigma}_1^{33} & * & * & * & * \\ \bar{\Sigma}_1^{41} & 0 & \bar{\Sigma}_1^{43} & \bar{\Sigma}_1^{44} & * & * & * \\ \bar{\Sigma}_1^{51} & 0 & \bar{\Sigma}_1^{53} & \bar{\Sigma}_1^{54} & \bar{\Sigma}_1^{55} & * & * \\ \bar{\Sigma}_1^{61} & 0 & \bar{\Sigma}_1^{63} & \bar{\Sigma}_1^{64} & \bar{\Sigma}_1^{65} & \bar{\Sigma}_1^{66} & * \\ \bar{\Sigma}_1^{71} & 0 & \bar{\Sigma}_1^{73} & 0 & 0 & 0 & \bar{\Sigma}_1^{77} \end{bmatrix}$$

$$\bar{\Pi}_2 = \begin{bmatrix} \bar{\Sigma}_2 & * \\ h\bar{F}_2 & \varkappa_2^2 \bar{R}_2 - 2\varkappa_2 X_{21} \end{bmatrix}, \bar{\Re}_2 = \begin{bmatrix} \bar{\bar{R}}_2 & * \\ \bar{U}_2 & \bar{\bar{R}}_2 \end{bmatrix}$$

$$\bar{\bar{R}}_1 = e^{-2\alpha_1 h}\begin{bmatrix} \bar{R}_1 & * \\ 0 & 3\bar{R}_1 \end{bmatrix}, \bar{U}_1 = \begin{bmatrix} \bar{U}_{11} & \bar{U}_{12} \\ \bar{U}_{13} & \bar{U}_{14} \end{bmatrix}$$

$$\bar{\bar{R}}_2 = \begin{bmatrix} \bar{R}_2 & * \\ 0 & 3\bar{R}_2 \end{bmatrix}, \bar{U}_2 = \begin{bmatrix} \bar{U}_{21} & \bar{U}_{22} \\ \bar{U}_{23} & \bar{U}_{24} \end{bmatrix}$$

$$\bar{\Sigma}_1^{11} = 2\alpha_1 X_{11} + \mathrm{He}(AX_{11}) + \bar{Q}_1 - 4e^{-2\alpha_1 h}\bar{R}_1$$

$$\bar{\Sigma}_1^{21} = C^T T_1^T, \bar{\Sigma}_1^{22} = 2\alpha_1 X_{12} + \mathrm{He}(AX_{12} - T_1 C)$$

$$\bar{\Sigma}_1^{31} = Y^T B^T - 2e^{-2\alpha_1 h}\bar{R}_1 - \bar{U}_{11} - \bar{U}_{12} - \bar{U}_{13} - \bar{U}_{14}$$

$$\bar{\Sigma}_1^{33} = \varepsilon\bar{\Omega} - 8e^{-2\alpha_1 h}\bar{R}_1 + \mathrm{He}\big(\bar{U}_{11} - \bar{U}_{12} + \bar{U}_{13} - \bar{U}_{14}\big)$$

$$\bar{\Sigma}_1^{41} = \bar{U}_{11} + \bar{U}_{12} - \bar{U}_{13} - \bar{U}_{14}$$

$$\bar{\Sigma}_1^{43} = -2e^{-2\alpha_1 h}\bar{R}_1 - \bar{U}_{11} + \bar{U}_{12} + \bar{U}_{13} - \bar{U}_{14}$$

$$\bar{\Sigma}_1^{44} = -e^{-2\alpha_1 h}\bar{Q}_1 - 4e^{-2\alpha_1 h}\bar{R}_1, \bar{\Sigma}_1^{51} = 6e^{-2\alpha_1 h}\bar{R}_1$$

$$\bar{\Sigma}_1^{53} = 6e^{-2\alpha_1 h}\bar{R}_1 + 2\bar{U}_{12}^T + 2\bar{U}_{14}^T$$

$$\bar{\Sigma}_1^{54} = -2\bar{U}_{12}^T + 2\bar{U}_{14}^T, \bar{\Sigma}_1^{55} = -12e^{-2\alpha_1 h}\bar{R}_1$$

$$\bar{\Sigma}_1^{61} = 2\bar{U}_{13} + 2\bar{U}_{14}, \bar{\Sigma}_1^{63} = 6e^{-2\alpha_1 h}\bar{R}_1 - 2\bar{U}_{13} + 2\bar{U}_{14}$$

$$\bar{\Sigma}_1^{64} = 6e^{-2\alpha_1 h}\bar{R}_1, \bar{\Sigma}_1^{65} = -4\bar{U}_{14}, \bar{\Sigma}_1^{66} = -12e^{-2\alpha_1 h}\bar{R}_1$$

$$\bar{\Sigma}_1^{71} = Y^T B^T, \bar{\Sigma}_1^{73} = \varepsilon\bar{\Omega}, \bar{\Sigma}_1^{77} = (\varepsilon - 1)\bar{\Omega}$$

$$\bar{F}_1 = \begin{bmatrix} AX_{11} & T_1 C & BY & 0 & 0 & 0 & BY \end{bmatrix}$$

$$\bar{\Sigma}_2 = \begin{bmatrix} \bar{\Sigma}_2^{11} & * & * & * & * & * \\ \bar{\Sigma}_2^{21} & \bar{\Sigma}_2^{22} & * & * & * & * \\ \bar{\Sigma}_2^{31} & 0 & \bar{\Sigma}_2^{33} & * & * & * \\ \bar{\Sigma}_2^{41} & 0 & \bar{\Sigma}_2^{43} & \bar{\Sigma}_2^{44} & * & * \\ \bar{\Sigma}_2^{51} & 0 & \bar{\Sigma}_2^{53} & \bar{\Sigma}_2^{54} & \bar{\Sigma}_2^{55} & * \\ \bar{\Sigma}_2^{61} & 0 & \bar{\Sigma}_2^{63} & \bar{\Sigma}_2^{64} & \bar{\Sigma}_2^{65} & \bar{\Sigma}_2^{66} \end{bmatrix}$$

$$\bar{\Sigma}_2^{11} = -2\alpha_2 X_{21} + \mathrm{He}(AX_{21}) + \bar{Q}_2 - 4\bar{R}_2$$

$$\bar{\Sigma}_2^{21} = C^T T_2^T, \bar{\Sigma}_2^{22} = -2\alpha_2 X_{22} + \mathrm{He}(AX_{22} - T_2 C)$$

$$\bar{\Sigma}_2^{31} = -2\bar{R}_2 - \bar{U}_{21} - \bar{U}_{22} - \bar{U}_{23} - \bar{U}_{24}$$

$$\bar{\Sigma}_2^{33} = -8\bar{R}_2 + \mathrm{He}\big(\bar{U}_{21} - \bar{U}_{22} + \bar{U}_{23} - \bar{U}_{24}\big)$$

$$\bar{\Sigma}_2^{41} = \bar{U}_{21} + \bar{U}_{22} - \bar{U}_{23} - \bar{U}_{24}$$

$$\bar{\Sigma}_2^{43} = -2\bar{R}_2 - \bar{U}_{21} + \bar{U}_{22} + \bar{U}_{23} - \bar{U}_{24}$$

$$\bar{\Sigma}_2^{44} = -e^{2\alpha_2 h}\bar{Q}_2 - 4\bar{R}_2$$

$$\bar{\Sigma}_2^{61} = 2\bar{U}_{23} + 2\bar{U}_{24}, \bar{\Sigma}_2^{63} = 6\bar{R}_2 - 2\bar{U}_{23} + 2\bar{U}_{24}$$

$$\bar{\Sigma}_2^{64} = 6\bar{R}_2, \bar{\Sigma}_2^{65} = -4\bar{U}_{24}, \bar{\Sigma}_2^{66} = -12\bar{R}_2$$

$$\bar{F}_2 = \begin{bmatrix} AX_{21} & T_2 C & 0 & 0 & 0 & 0 \end{bmatrix}$$

then the switched system (18) with

$$L_1 = T_1\bar{X}_{12}^{-1}, L_2 = T_2\bar{X}_{22}^{-1}, K = YX_{11}^{-1}$$

is GES in the presence of the periodic DoS jamming attacks (2).

Proof: See Appendix C. ■

Remark 8: It should be pointed out that Theorem 2 is closely related to the sampling period h. From (13), it is seen that the upper bound of the artificial time-varying delay function $\tau_{k,n}(t)$ is dependent on h. Thus, Theorem 2 is a delay-dependent condition for event-triggered observed-based controllers. For a larger h, it is more likely that Theorem 2 fails to obtain the controller design. On the other hand, a smaller h usually results in better performance of the resulting closed-loop system under consideration while increasing the network loads. Therefore, in using the proposed method, due to the fact that the event-triggering mechanism can reduce the network loads greatly, one should choose a small h to design a suitable event-triggered observed-based controllers such that the resulting closed-loop system can achieve the desired system performance, which can be seen from the simulation section.

Remark 9: Theorem 2 establishes the existence condition of a resilient event-triggering scheme (5) and an event-triggered observer (3) with DoS jamming attacks (2). Specifically, if there exists a feasible solution of the matrix inequalities (31)–(38), then resilient event-triggering scheme (5) and the observer (3) can be designed simultaneously. Notice from (29) and (30) that ρ and J^* are monotonic increasing functions of α_1, and are monotonic decreasing functions of α_2, μ_1, and μ_2. In view of this, if the matrix inequalities (31)–(38) are feasible, α_1 should be chosen as large as possible while α_2, μ_1, and μ_2 should be chosen as small as possible to get large values of ρ and J^*. On the other hand, from (31)–(38), it is seen that a smaller α_1 and larger values of α_2, μ_1, and μ_2 are beneficial to the solvability of the inequalities (31)–(38). Therefore, one can use an iterative algorithm (see below) to obtain the maximal value of α_1, and the minimal values of α_2, μ_1, and μ_2 that guarantee the feasibility of the inequalities (31)–(38).

Step 1: Take a small initial value of $\alpha_1 > 0$ such that the inequality (31) is feasible. Specify an iteration step-size $\Delta\alpha_1 > 0$ for α_1.

Step 2: Set $\alpha_1 = \alpha_1 + \Delta\alpha_1$.

Step 3: Checking the feasibility of the inequality (31). If the inequality (31) is feasible, go to step 2. Otherwise, exit and set $\alpha_1 = \alpha_1 - \Delta\alpha_1$.

Step 4: Following some similar procedures as in steps 1–3 to obtain the minimal $\alpha_2 > 0$.

Step 5: For the obtained maximal α_1, minimal α_2, taking a large initial $\mu_1 > 0$ such that (34), (37), and (38) are feasible. Specify an iteration step-size $\Delta\mu_1 > 0$ for μ_1.

Step 6: Set $\mu_1 = \mu_1 - \Delta\mu_1$.

Step 7: Checking the feasibility of (34), (37), and (38). If these inequalities are feasible, then go to step 6. Otherwise, exit and set $\mu_1 = \mu_1 + \Delta\mu_1$.

Step 8: Following some similar procedures as in steps 5–7 to obtain the minimal $\mu_2 > 0$.

Step 9: Take the values of $T_{\text{off}}^{\min}$ and T satisfying $0 < T_{\text{off}}^{\min} < T$ and inequality (22). It ends.

Remark 10: Recently, a remarkable work on observer-based ETC strategy under DoS attacks was reported in [41]. However, this paper is different from [41] in several aspects. First, a pure discrete-time setting is considered in [41], while a sampled-data networked linear continuous-time system is discussed in this paper. Second, the considered DoS attack model and the proposed event-triggering mechanism along with modeling method are also different, which allows us to analyze stability using a piecewise Lyapunov functional method from [38] instead of a common quadratic Lyapunov function as in [41]. It is also noted that an alternative approach to co-design of controller and observer gain matrices under DoS attacks is developed in this paper.

Remark 11: Note that in the elegant work of Feng and Tesi [30], it is shown that finite-time observer-based controllers are indeed advantageous compared to generic dynamic compensators since they can maximize the amount of DoS attacks that the control system can tolerate. In this paper, there are two major advantages of using the observer-based controller compared to a generic dynamic compensator. First, the generic dynamic compensator works in the entire process and wastes some computation and network resources to some extent, while the observer-based controller can guarantee the satisfactory system performance with shorter control task execution time despite the presence of the DoS attacks, which can be seen from Figs. 3–5 in simulation. Second, the generic dynamic compensators fail to work when the actuator channel is subject to DoS attacks, while the proposed observer-based controller can still work well.

Remark 12: It is worth pointing out that the main difficulties to get stability with a pure event-triggered strategy lie in that how to guarantee a positive lower bound on the interevent time interval generated by events under the designed event-triggering condition (i.e., excluding the Zeno phenomenon). In general, in order to proof the existence of the positive lower bound of the interevent time interval, we usually need complicated calculations by adopting the method proposed in [11] or make an assumption that there exists a positive lower bound for the interevent time as in [28]. Different from these works, this paper considers an event-triggered strategy which prevents the occurrence of Zeno behavior by construction and removes most of the difficulties arising from stability analysis in pure event-triggered formulation.

IV. Application to Offshore Structure

In this section, a practical example is utilized to demonstrate the effectiveness of the proposed method. Let the physical plant in Fig. 1 be an offshore structure with an active mass damper (AMD) mechanisms, which is taken from [42]. The dynamic equations of the offshore structure are given by

$$\begin{cases} m_1\ddot{z}_1(t) = -c_1\dot{z}_1(t) - k_1z_1(t) + k_2z_2(t) \\ \qquad\qquad - k_2z_1(t) + c_2(\dot{z}_2(t) - \dot{z}_1(t)) - u(t) \\ m_2\ddot{z}_2(t) = -c_2(\dot{z}_2(t) - \dot{z}_1(t)) - k_2z_2(t) \\ \qquad\qquad + k_2z_1(t) + u(t) \end{cases} \tag{39}$$

where $z_1(t)$ and $z_2(t)$ are the displacements of the offshore structure and the AMD, respectively; m_1 and m_2 are the masses of the offshore structure and the AMD, respectively; k_1 and k_2 are the stiffnesses of the offshore structure and the AMD, respectively; c_1 and c_2 are the dampings of the offshore structure and the AMD, respectively; and $u(t)$ is the control force of the system. Note that here, for simplicity, the wave force acting on the offshore structure is overlooked.

Define $x_1(t) = z_1(t)$, $x_2(t) = z_2(t)$, $x_3(t) = \dot{z}_1(t)$, $x_4(t) = \dot{z}_2(t)$, and $x(t) = \begin{bmatrix} x_1(t) & x_2(t) & x_3(t) & x_4(t) \end{bmatrix}^T$, and assume the controlled outputs are the displacements of the offshore structure and the AMD. Thus, the state-space representation of the above (39) can be written as the form of the system (1) with

$$A = \begin{bmatrix} 0 & 0 & 1 & 0 \\ 0 & 0 & 0 & 1 \\ -\frac{k_1+k_2}{m_1} & \frac{k_2}{m_1} & -\frac{c_1+c_2}{m_1} & \frac{c_2}{m_1} \\ \frac{k_2}{m_2} & -\frac{k_2}{m_2} & \frac{c_2}{m_2} & -\frac{c_2}{m_2} \end{bmatrix}$$

$$B = \begin{bmatrix} 0 & 0 & -\frac{1}{m_1} & \frac{1}{m_2} \end{bmatrix}^T$$

$$C = \begin{bmatrix} 1 & 0 & 0 & 0 \\ 0 & 0 & 1 & 0 \end{bmatrix}.$$

As in [42], suppose that the offshore structure is placed in the water with depths $d_0 = 218$ m. The length L of the offshore structure is 249 m and the cylinder diameter $\tilde{D} = 1.83$ m. The masses, natural frequencies, and the damping ratios of the structure and AMD are given as $m_1 = 7\,825\,307$ kg, $\omega_1 = 2.0466$ rad/s, $\xi_1 = 2\%$, $m_2 = 78253$ kg, $\omega_2 = 2.00074$ rad/s, and $\xi_2 = 20\%$.

For this simplified model, in the following, we first co-design the event-triggering parameters (ε, Ω), control gain matrix K in (6), and observer gain matrices L_1 and L_2 in (3) such that the closed-loop system (18) is GES. To this end, we assume the jammer, imposing jamming signal $\mathcal{I}_{\mathrm{DoS}}(t)$ (2) with $T = 2$ s and $T_{\mathrm{off}}^{\min} = 1.6$ s. Choosing $\mu_1 = 1.1$, $\mu_2 = 1.1$, $\alpha_1 = 0.2$, $\alpha_2 = 0.45$, and $h = 0.02$ s satisfying (22). For given $\varepsilon = 0.3$, $\varkappa_1 = 1$, $\varkappa_2 = 1$, $\varpi_1 = 5$, and $\varpi_2 = 5$ solving the LMIs in Theorem 2, it is found that the observer-based ETC problem is feasible, and the obtained event-triggering parameter Ω, the controller gain matrix K, and the observer gain matrices L_1 and L_2 are given by

$$\Omega = 10^3 \times \begin{bmatrix} 8.1471 & -0.0298 & -0.2453 & -0.1394 \\ -0.0298 & 0.0003 & 0.0023 & 0.0006 \\ -0.2453 & 0.0023 & 0.0232 & 0.0045 \\ -0.1394 & 0.0006 & 0.0045 & 0.0025 \end{bmatrix} \tag{40}$$

$$K = 10^6 \times \begin{bmatrix} 4.3841 & -0.0145 & -0.1253 & -0.0709 \end{bmatrix} \tag{41}$$

$$\begin{cases} L_1 = \begin{bmatrix} -0.0098 & -0.0034 \\ 0.2021 & 0.2484 \\ 0.0151 & 0.0005 \\ -1.6683 & -0.4939 \end{bmatrix} \\ L_2 = \begin{bmatrix} 0.1746 & -0.0226 \\ -0.8664 & 1.4365 \\ 0.1470 & 0.4244 \\ -4.8470 & -1.3500 \end{bmatrix}. \end{cases} \tag{42}$$

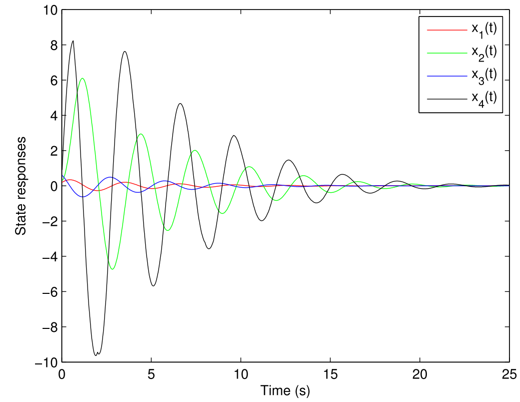

Fig. 2. State responses of the system with $T = 2$ s and $T_{\mathrm{off}}^{\min} = 1.6$ s.

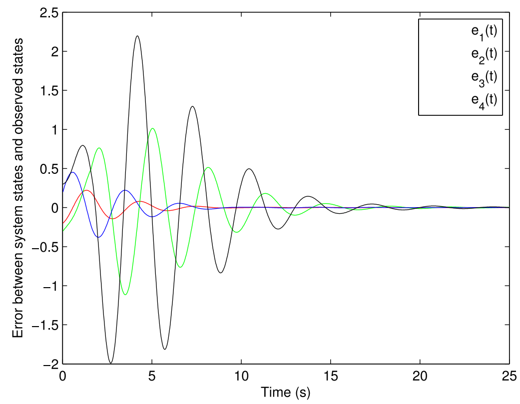

Fig. 3. Error responses between system states and observed states with $T = 2$ s and $T_{\mathrm{off}}^{\min} = 1.6$ s.

Simulations are carried out by connecting the observer-based event-triggered state-feedback controller (6) with (40) to the offshore structure under the event-triggering mechanism (5) with (40) in the presence of the periodic DoS jamming attack (2) with $T = 2$ s and $T_{\mathrm{off}}^{\min} = 1.6$ s. The initial conditions are taken as $x_0 = \begin{bmatrix} 0.2 & 0.3 & 0.6 & 0.9 \end{bmatrix}^T$ and $\hat{x}_0 = \begin{bmatrix} 0.4 & 0.6 & 0.4 & 0.6 \end{bmatrix}^T$ and the simulation time is assumed to be 25 s.In the presence of DoS attacks, the state responses of the considered system, the error between system states and observed states, the release time intervals between any two consecutive release instants, and the control input are depicted in Figs. 2–5, respectively, from which we can see that: 1) the observer-based error system is exponentially stable; 2) the proposed resilient event-triggering mechanism can reduce the amount of control updates; and 3) the observer-based resilient event-triggered state-feedback controller does have counteracted the effect of the periodic jamming attacks.

In order to show the influence of the jamming period T, we solve the following optimization problem for different values of T in the time interval [0, 25 s] (the parameters μ_1, μ_2, α_1, α_2, ε, h, $\varkappa_1$, $\varkappa_2$, ϖ_1, and ϖ_2 are chosen as the same before)

$$\bar{T}_{\mathrm{off}}^{\min} = \min\Big\{ T_{\mathrm{off}}^{\min} \,|\, T_{\mathrm{off}}^{\min} \text{ satisfying (22) subjects to (31)–(38)} \Big\}. \tag{43}$$

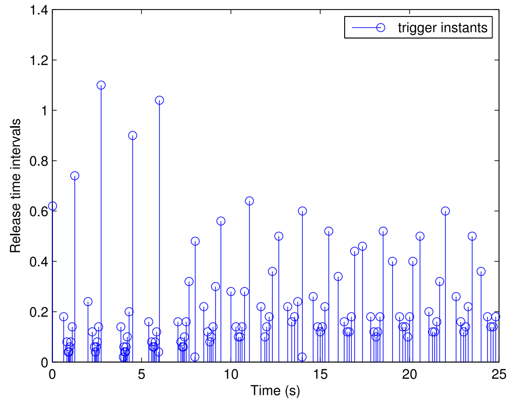

Fig. 4. Release time intervals with $T = 2$ s and $T_{\rm off}^{\min} = 1.6$ s.

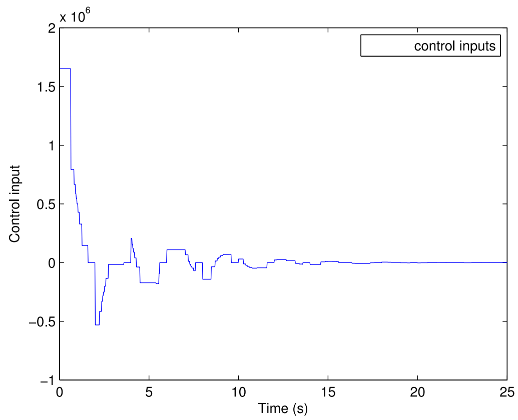

Fig. 5. Control input with $T = 2$ s and $T_{\rm off}^{\min} = 1.6$ s.

TABLE I
$\bar{T}_{\rm off}^{\min}$, $\bar{J}$, AND J^* FOR DIFFERENT VALUES OF T

T	2	3	5	7	9
$\bar{T}_{off}^{\min}$	1.56	2.25	3.63	5.02	6.40
T_{off}^{*}	1.55	2.24	3.63	5.01	6.40
$\bar{J}$	22%	25%	27.4%	28.3%	28.9%
J^*	22.44%	25.21%	27.44%	28.39%	28.92%

Table I shows the minimum $T_{\rm off}^{\min}$ for which the exponential stability of the closed-loop system under consideration is guaranteed, the MAJA denoted by $\bar{J} \triangleq [(T-\bar{T}_{\rm off}^{\min})/T] \times 100\%$ and the corresponding upper bound of $\bar{J}$ obtained for each T chosen. From Table I, it can be seen that when T increases, the values of $\bar{T}_{\rm off}^{\min}$ and $\bar{J}$ also increase. This may be reasonable because for a larger jammer period T, the shortest time the jammer sleeps should also be larger to make the system stable correspondingly. In other words, the system can relatively tolerate more malicious attacks as well. Furthermore, it is observed that the obtained lower bound $\bar{T}_{\rm off}^{\min}$ of $T_{\rm off}^{\min}$ [solving (43) by iteration] is very close to its analytical bound $T_{\rm off}^{*}$, which demonstrates the reasonability of Remark 4. In addition, the obtained MAJA $\bar{J}$ is always smaller than J^*, which illustrates the validity of Remark 6.

In what follows, in order to show the relationship between $\bar{T}_{\rm off}^{\min}$ and the decay rate ρ, some calculations are listed in Table II. It is observed that the bigger the $\bar{T}_{\rm off}^{\min}$, the larger the ρ, which validates the statement of Remark 4.

TABLE II
λ AND ρ FOR DIFFERENT VALUES OF $T_{\rm off}^{\min}$

$T_{off}^{\min}$	1.56	1.66	1.76	1.86	1.96
λ	0.0114	0.1414	0.2714	0.4014	0.5314
ρ	0.0028	0.0353	0.0678	0.1003	0.1328

TABLE III
$h_{\max}$ AND $\bar{T}_{\rm off}^{\min}$ FOR DIFFERENT VALUES OF σ

ε	0.3	0.2	0.1	0.05	0.01
h_{max}	0.07	0.12	0.15	0.17	0.18
$\bar{T}_{off}^{\min}$	1.47	1.52	1.55	1.57	1.58

To further show the effect of the triggering parameter ε on the stability of the system, we assume that $\mu_1 = 1.01$, $\mu_2 = 1.01$, $\alpha_1 = 0.2$, $\alpha_2 = 0.45$, $T = 2$, $T_{\rm off}^{\min} = 1.6$, and $\varkappa_1$, $\varkappa_2$, ϖ_1, and ϖ_2 are chosen as the same above. The maximum allowable sampling period $h_{\max}$ and the corresponding $\bar{T}_{\rm off}^{\min}$ for different ε are listed in Table III. From Table III, we find that for given the DoS attacks, $h_{\max}$ and $\bar{T}_{\rm off}^{\min}$ are becoming bigger when the triggering parameter ε is decreasing. Hence, there exists a tradeoff between system performance and resource occupancy.

V. CONCLUSION

In this paper, we have investigated the observer-based ETC for a class of networked linear systems under periodic DoS jamming attacks. A novel resilient event-triggered communication mechanism has been proposed to enhance the utilization efficiency of network resources while resisting the DoS jamming attacks. Inspired by the intermittent property of the DoS jamming attacks, a new switched observer error system model has been established, which facilitates us to consider the effects of the resilient event-triggered strategy and DoS jamming attacks in a unified framework. Tractable LMI-based stability analysis and control design criteria for the co-design of the observer and controller gains have been derived while preserving satisfactory control performance despite the presence of DoS jamming attacks. At last, a practical example has been exploited to demonstrate the effectiveness of the proposed resilient event-triggered controller design method.

In our future work, we will extend the proposed method to deal with the event-based H_∞ filtering/fault detection problem and event-based adaptive control problem in the presence of DoS jamming attacks with the help of [43]–[45]. Besides, how to extend the proposed framework to study the event-triggered NCSs under more general DoS attacks is another interesting research venue, where the attack signals are unknown and happen aperiodically.

APPENDIX A
PROOF OF LEMMA 1

Construct the following piecewise Lyapunov functional for system (18):

$$V(t) = \begin{cases} V_1(t), & t \in \Upsilon_{k,n} \cap \bar{\mathcal{L}}_{1,n}, k \in K(n) \\ V_2(t), & t \in \bar{\mathcal{L}}_{2,n}, n \in \mathbb{N} \end{cases} \quad (44)$$

where

$$\begin{aligned} V_1(t) &= \xi^T(t)P_1\xi(t) \\ &+ \int_{t-h}^{t} \xi^T(s)\rho_1(s)G^TQ_1G\xi(s)ds \\ &+ h\int_{-h}^{0}\int_{t+\theta}^{t} \dot{\xi}^T(s)\rho_1(s)G^TR_1G\dot{\xi}(s)dsd\theta \end{aligned}$$

and

$$\begin{aligned} V_2(t) &= \xi^T(t)P_2\xi(t) \\ &+ \int_{t-h}^{t} \xi^T(s)\rho_2(s)G^TQ_2G\xi(s)ds \\ &+ h\int_{-h}^{0}\int_{t+\theta}^{t} \dot{\xi}^T(s)\rho_2(s)G^TR_2G\dot{\xi}(s)dsd\theta. \end{aligned}$$

where $P_1 \in \mathbb{R}^{2n\times 2n}$, $Q_1 \in \mathbb{R}^{n\times n}$, $R_1 \in \mathbb{R}^{n\times n}$, $P_2 \in \mathbb{R}^{2n\times 2n}$, $Q_2 \in \mathbb{R}^{n\times n}$, $R_2 \in \mathbb{R}^{n\times n}$, and $\Omega \in \mathbb{R}^{n\times n}$ are the symmetric positive definite matrices. We now consider the following two cases.

Case 1: $\forall t \in \Upsilon_{k,n} \cap \bar{\mathcal{L}}_{1,n}$, $\forall k \in K(n)$, $n \in \mathbb{N}$, taking the derivative of $V(t)$ with respect to t along the system (18) yields

$$\begin{aligned} \dot{V}(t) \le& -2\alpha_1V(t) + 2\alpha_1\xi^T(t)P_1\xi(t) + \xi^T(t)P_1\dot{\xi}(t) \\ &+ \dot{\xi}^T(t)P_1\xi(t) + \xi^T(t)G^TQ_1G\xi(t) \\ &- \xi^T(t-h)e^{-2\alpha_1h}G^TQ_1G\xi(t-h) \\ &+ h^2\dot{\xi}^T(t)G^TR_1G\dot{\xi}(t) \\ &- h\int_{t-h}^{t}\dot{\xi}^T(s)e^{-2\alpha_1h}G^TR_1G\dot{\xi}(s)ds. \end{aligned} \tag{45}$$

Note that

$$\begin{aligned} &-h\int_{t-h}^{t}\dot{\xi}^T(s)G^TR_1G\dot{\xi}(s)ds \\ &= -h\int_{t-\tau_{k,n}(t)}^{t}\dot{\xi}^T(s)G^TR_1G\dot{\xi}(s)ds \\ &\quad - h\int_{t-h}^{t-\tau_{k,n}(t)}\dot{\xi}^T(s)G^TR_1G\dot{\xi}(s)ds. \end{aligned} \tag{46}$$

Using the inequality in [46] and [47], we obtain

$$\begin{cases} -h\int_{t-\tau_{k,n}(t)}^{t}\dot{\xi}^T(s)e^{-2\alpha_1h}G^TR_1G\dot{\xi}(s)ds \\ \quad \le -\frac{h}{\tau_{k,n}(t)}\Lambda_1^T\tilde{R}_1\Lambda_1 \\ -h\int_{t-h}^{t-\tau_{k,n}(t)}\dot{\xi}^T(s)e^{-2\alpha_1h}G^TR_1G\dot{\xi}(s)ds \\ \quad \le -\frac{h}{h-\tau_{k,n}(t)}\Lambda_2^T\tilde{R}_1\Lambda_2 \end{cases} \tag{47}$$

where $\Lambda_1 = \mathrm{diag}\{G,G\}\big[\upsilon_{11}^T \quad \upsilon_{12}^T\big]^T$, $\upsilon_{11} = \xi(t) - \xi(t-\tau_{k,n}(t))$, $\upsilon_{12} = \xi(t) + \xi(t-\tau_{k,n}(t)) - 2\delta_1(t)$, $\delta_1(t) = \int_{t-\tau_{k,n}(t)}^{t}[\xi(s)/(\tau_{k,n}(t))]ds$, $\Lambda_2 = \mathrm{diag}\{G,G\}\big[\upsilon_{21}^T \quad \upsilon_{22}^T\big]^T$, $\upsilon_{21} = \xi(t-\tau_{k,n}(t)) - \xi(t-h)$, $\upsilon_{22} = \xi(t-\tau_{k,n}(t)) + \xi(t-h) - 2\delta_2(t)$, and $\delta_2(t) = \int_{t-h}^{t-\tau_{k,n}(t)}[\xi(s)/(h-\tau_{k,n}(t))]ds$.

Using (46) and (47) to deal with integral terms in (45) by [46, Lemma 3], we have

$$-h\int_{t-h}^{t}\dot{\xi}^T(s)e^{-2\alpha_1h}G^TR_1G\dot{\xi}(s)ds \le -\Lambda_3^T\Re_1\Lambda_3 \tag{48}$$

where $\Lambda_3 = \mathrm{diag}\{G,G,G,G\}\big[\upsilon_{11}^T \quad \upsilon_{12}^T \quad \upsilon_{21}^T \quad \upsilon_{22}^T\big]^T$.

Substituting (48) into (45), adding the terms $e_{k,n}^T(t)\Omega e_{k,n}(t) - e_{k,n}^T(t)\Omega e_{k,n}(t)$ to the right-hand side of (45), and using the event-triggering condition (15) to bound the term $e_{k,n}^T(t)\Omega e_{k,n}(t)$, we have

$$\begin{aligned} \dot{V}(t) \le& -2\alpha_1V(t) \\ &+ \eta_1^T(t)\Big[\Sigma_1 + h^2F_1^TG^TR_1GF_1\Big]\eta_1(t) \end{aligned} \tag{49}$$

where

$$\begin{aligned} \eta_1^T(t) = \big[\,&\xi^T(t) \quad \xi^T\big(t-\tau_{k,n}(t)\big)G^T \quad \xi^T(t-h)G^T \\ &\delta_1^T(t)G^T \quad \delta_2^T(t)G^T \quad e_{k,n}^T(t)\,\big]. \end{aligned}$$

Taking the Schur complement of the matrix $\Pi_1 < 0$ in (19), we obtain that $\Sigma_1 + h^2F_1^TG^TR_1GF_1 < 0$, which implies that

$$\dot{V}(t) \le -2\alpha_1V(t). \tag{50}$$

Due to the arbitrary of k, it follows that $\forall t \in \bar{\mathcal{L}}_{1,n}$:

$$V(t) \le e^{-2\alpha_1(t-nT)}V(nT). \tag{51}$$

Case 2: Following the similar arguments as the ones in the proof of case 1, the differential of $V(t)$ with respect to $t \in \bar{\mathcal{L}}_{2,n}$ along the trajectory of system (18) yields

$$\begin{aligned} \dot{V}(t) \le& 2\alpha_2V(t) \\ &+ \eta_2^T(t)\Big[\Sigma_2 + h^2F_2^TG^TR_2GF_2\Big]\eta_2(t) \end{aligned} \tag{52}$$

where

$$\begin{aligned} \eta_2^T(t) = \big[\,&\xi^T(t) \quad \xi^T\big(t-\tau_{k,n}(t)\big)G^T \\ &\xi^T(t-h)G^T \quad \delta_1^T(t)G^T \quad \delta_2^T(t)G^T\,\big]. \end{aligned}$$

According to the condition $\Pi_2 < 0$ in (20), we obtain that $\Sigma_2 + h^2F_2^TG^TR_2GF_2 < 0$, which implies that $\forall t \in \bar{\mathcal{L}}_{2,n}$

$$V(t) \le e^{2\alpha_2\left(t-nT-T_{\mathrm{off}}^{\min}\right)}V\Big(nT + T_{\mathrm{off}}^{\min}\Big). \tag{53}$$

From the above analysis of cases 1 and 2, the conditions (19) and (20) guarantee the inequality (21) is satisfied. The proof is thus completed.

Appendix B
Proof of Theorem 1

Choose a piecewise Lyapunov functional $V(t)$ as Lemma 1. According to (23)–(28), it follows from Lemma 1 that:

$$\begin{aligned} V_1(nT) &= \xi^T(nT)P_1\xi(nT) \\ &+ \int_{nT-h}^{nT}\xi^T(s)e^{-2\alpha_1(nT-s)}G^TQ_1G\xi(s)ds \\ &+ h\int_{-h}^{0}\int_{nT+\theta}^{nT}\dot{\xi}^T(s)e^{-2\alpha_1(nT-s)}G^T \\ &\times R_1G\dot{\xi}(s)dsd\theta \\ &\le \mu_2V_2\big(nT^-\big). \end{aligned} \tag{54}$$

Similarly,

$$V_2\Big(nT + T_{\mathrm{off}}^{\min}\Big) \le \mu_1e^{2(\alpha_1+\alpha_2)h}V_1\Big[\Big(nT + T_{\mathrm{off}}^{\min}\Big)^-\Big]. \tag{55}$$

In the sequel, using (21), (54), and (55), by induction, when $t \in [nT, nT + T_{\text{off}}^{\min})$, one has

$$\begin{aligned} V_1(t) &\le (\mu_1\mu_2)^n e^{-2n\alpha_1 T_{\text{off}}^{\min}} \\ &\quad \times e^{2n\alpha_2(T - T_{\text{off}}^{\min})} \\ &\quad \times e^{2n(\alpha_1+\alpha_2)h} V_1(0) \\ &= e^{-\lambda n} V_1(0) \\ V_1\left[\left(nT + T_{\text{off}}^{\min}\right)^-\right] &\le (\mu_1\mu_2)^n e^{-2n\alpha_1 T_{\text{off}}^{\min}} \\ &\quad \times e^{2n\alpha_2(T - T_{\text{off}}^{\min})} \\ &\quad \times e^{2n(\alpha_1+\alpha_2)h} \\ &\quad \times e^{-2\alpha_1 T_{\text{off}}^{\min}} V_1(0). \end{aligned} \tag{56}$$

Note that

$$nT \le t \le nT + T_{\text{off}}^{\min} \implies \frac{t - T_{\text{off}}^{\min}}{T} < n \le \frac{t}{T}. \tag{57}$$

Combining (56) and (57), we obtain

$$V(t) \le V_1(0) e^{\frac{\lambda T_{\text{off}}^{\min}}{T}} e^{-\frac{\lambda}{T}t}. \tag{58}$$

On the other hand, when $t \in [nT + T_{\text{off}}^{\min}, (n+1)T)$, it follows from (22) that:

$$\begin{aligned} V_2(t) &\le \frac{(\mu_1\mu_2)^{n+1}}{\mu_2} e^{\left(-2\alpha_1 T_{\text{off}}^{\min} + 2\alpha_2(T - T_{\text{off}}^{\min}) + 2(\alpha_1+\alpha_2)h\right)n} \\ &\quad \times e^{-2\alpha_1 T_{\text{off}}^{\min} + 2\alpha_2(T - T_{\text{off}}^{\min}) + 2(\alpha_1+\alpha_2)h} V_1(0) \\ &= \frac{1}{\mu_2} e^{-\lambda(n+1)} V_1(0). \end{aligned} \tag{59}$$

Note that

$$nT + T_{\text{off}}^{\min} \le t < (n+1)T \;\Rightarrow\; \frac{t}{T} < n+1. \tag{60}$$

Combining (59) and (60), we have

$$V(t) \le \frac{V_1(0)}{\mu_2} e^{-\frac{\lambda}{T}t}. \tag{61}$$

Let $\zeta_1 = \min\{\lambda_{\min}(P_1), \lambda_{\min}(P_2)\}$, $\zeta_2 = \lambda_{\max}(P_1)$, $\zeta_3 = \zeta_2 + h\lambda_{\max}(Q_1) + (h^3/2)\lambda_{\max}(R_1)$, $\kappa = \sqrt{(\chi\zeta_3/\zeta_1)}$, and $\chi = \max\{e^{[(\lambda T_{\text{off}}^{\min})/T]}, (1/\mu_2)\}$. From (58) and (61), we obtain

$$V(t) \le \chi e^{-\frac{\lambda}{T}t} V_1(0). \tag{62}$$

From the definition of $V(t)$, it is not difficult to derive

$$V(t) \ge \zeta_1 \|\xi(t)\|^2,\; V_1(0) \le \zeta_3 \|\phi_0\|_h^2. \tag{63}$$

Combining (62) and (63), we have

$$\|\xi(t)\| \le \kappa e^{-\rho t} \|\phi_0\|_h,\;\; t \ge 0 \tag{64}$$

which proves that the system (18) is GES with decay rate ρ by Definition 1.

APPENDIX C
PROOF OF THEOREM 2

Set $P_1 = \begin{bmatrix} P_{11} & * \\ 0 & P_{12} \end{bmatrix}$, $P_2 = \begin{bmatrix} P_{21} & * \\ 0 & P_{22} \end{bmatrix}$ and define $X_{11} = P_{11}^{-1}$, $X_{12} = P_{12}^{-1}$, $X_{21} = P_{21}^{-1}$, $X_{22} = P_{22}^{-1}$, $X_{11}Q_1X_{11} = \bar{Q}_1$, $X_{11}R_1X_{11} = \bar{R}_1$, $X_{21}Q_2X_{21} = \bar{Q}_2$, $X_{21}R_2X_{21} = \bar{R}_2$, $X_{11}\Omega X_{11} = \bar{\Omega}$, $X_{11}U_{11}X_{11} = \bar{U}_{11}$, $X_{11}U_{12}X_{11} = \bar{U}_{12}$, $X_{11}U_{13}X_{11} = \bar{U}_{13}$, $X_{11}U_{14}X_{11} = \bar{U}_{14}$, $X_{21}U_{21}X_{21} = \bar{U}_{21}$, $X_{21}U_{22}X_{21} = \bar{U}_{22}$, $X_{21}U_{23}X_{21} = \bar{U}_{23}$, $X_{21}U_{24}X_{21} = \bar{U}_{24}$, and $Y = KX_{11}$, $T_1 = L_1\bar{X}_{12}$, $T_2 = L_2\bar{X}_{22}$. For $X_{12} = W\begin{bmatrix} X_{121} & * \\ 0 & X_{122} \end{bmatrix}W^T$ and $X_{22} = W\begin{bmatrix} X_{221} & * \\ 0 & X_{222} \end{bmatrix}W^T$. On the basis of [48, Lemma 2], there exist $\bar{X}_{12} = OSX_{121}S^{-1}O^T$, $\bar{X}_{22} = OSX_{221}S^{-1}O^T$ such that $CX_{12} = \bar{X}_{12}C$ and $CX_{22} = \bar{X}_{22}C$. Define $J_1 = \mathrm{diag}\{X_{11}, X_{12}, X_{11}, X_{11}, X_{11}, X_{11}, X_{11}, R_1^{-1}\}$ and $J_2 = \mathrm{diag}\{X_{21}, X_{22}, X_{21}, X_{21}, X_{21}, X_{21}, R_2^{-1}\}$. Then pre- and post-multiply J_1 and its transpose on both sides of (19), pre- and post-multiply J_2 and its transpose on both sides of (20). Furthermore, pre- and post-multiply (23) and (24) by $X_2 = \begin{bmatrix} X_{21} & * \\ 0 & X_{22} \end{bmatrix}$ and $X_1 = \begin{bmatrix} X_{11} & * \\ 0 & X_{12} \end{bmatrix}$, respectively, and using the Schur complement one can obtain (33) and (34). Utilizing the similar technique, pre- and post-multiplying (25) and (26) by X_{21} and (27) and (28) by X_{11}, respectively, and applying the inequalities $-X_{11}\bar{R}_1^{-1}X_{11} \le \varkappa_1^2\bar{R}_1 - 2\varkappa_1X_{11}$, $-X_{21}\bar{R}_2^{-1}X_{21} \le \varkappa_2^2\bar{R}_2 - 2\varkappa_2X_{21}$, $-X_{11}\bar{Q}_1^{-1}X_{11} \le \varpi_1^2\bar{Q}_1 - 2\varpi_1X_{11}$, and $-X_{21}\bar{Q}_2^{-1}X_{21} \le \varpi_2^2\bar{Q}_2 - 2\varpi_2X_{21}$ and the Schur complement one can derive (35)–(38). This completes the proof.

REFERENCES

[1] J. Y. Keller, K. Chabir, and D. Sauter, "Input reconstruction for networked control systems subject to deception attacks and data losses on control signals," *Int. J. Syst. Sci.*, vol. 47, no. 4, pp. 814–820, 2016.

[2] S. Amin, A. A. Cárdenas, and S. S. Sastry, "Safe and secure networked control systems under denial-of-service attacks," in *Proc. Int. Conf. Hybrid Syst. Comput. Control*, 2009, pp. 31–45.

[3] Z. H. Pang, G. P. Liu, and Z. Dong, "Secure networked control systems under denial of service attacks," *Proc. IFAC Vol.*, vol. 44, no. 1, pp. 8908–8913, 2011.

[4] L. Hu, Z. Wang, Q.-L. Han, and X. Liu, "State estimation under false data injection attacks: Security analysis and system protection," *Automatica*, vol. 87, pp. 176–183, Jan. 2018.

[5] V. S. Dolk, P. Tesi, C. D. Persis, and W. P. M. H. Heemels, "Event-triggered control systems under denial-of-service attacks," *IEEE Trans. Control Netw. Syst.*, vol. 4, no. 1, pp. 93–105, Mar. 2017.

[6] D. Ding, Z. Wang, Q.-L. Han, and G. Wei, "Security control for discrete-time stochastic nonlinear systems subject to deception attacks," *IEEE Trans. Syst., Man, Cybern., Syst.*, vol. 48, no. 5, pp. 779–789, May 2018.

[7] S. Xiao, Q.-L. Han, X. Ge, and Y. Zhang, "Secure distributed finite-time filtering for positive systems over sensor networks under deception attacks," *IEEE Trans. Cybern.*, to be published. doi: 10.1109/TCYB.2019.2900478.

[8] W. Xu, W. Trappe, Y. Zhang, and T. Wood, "The feasibility of launching and detecting jamming attacks in wireless networks," in *Proc. ACM Int. Symp. Mobile Ad Hoc Netw. Comput.*, 2005, pp. 46–57.

[9] D. Ding, Q.-L. Han, Y. Xiang, X. Ge, and X.-M. Zhang, "A survey on security control and attack detection for industrial cyber-physical systems," *Neurocomputing*, vol. 275, pp. 1674–1683, Jan. 2018.

[10] P. Millán, L. Orihuela, I. Jurado, and F. R. Rubio, "Formation control of autonomous underwater vehicles subject to communication delays," *IEEE Trans. Control Syst. Technol.*, vol. 22, no. 2, pp. 770–777, Mar. 2014.

[11] P. Tabuada, "Event-triggered real-time scheduling of stabilizing control tasks," *IEEE Trans. Autom. Control*, vol. 52, no. 9, pp. 1680–1685, Sep. 2007.

[12] X. Wang and M. D. Lemmon, "Event-triggering in distributed networked control systems," *IEEE Trans. Autom. Control*, vol. 56, no. 3, pp. 586–601, Mar. 2011.

[13] X.-M. Zhang and Q.-L. Han, "Event-based H_∞ control for a class of nonlinear networked control systems using novel integral inequalities," *Int. J. Robust Nonlinear Control*, vol. 27, no. 4, pp. 679–700, 2017.

[14] D. Zhang, Q.-L. Han, and X. Jia, "Network-based output tracking control for T–S fuzzy systems using an event-triggered communication scheme," *Fuzzy Sets Syst.*, vol. 273, pp. 26–48, Aug. 2015.

[15] X. You, C. C. Hua, and X. P. Guan, "Event-triggered leader-following consensus for nonlinear multiagent systems subject to actuator saturation using dynamic output feedback method," *IEEE Trans. Autom. Control*, vol. 63, no. 12, pp. 4391–4396, Dec. 2018.

[16] X. You, C. C. Hua, and X. P. Guan, "Self-triggered leader-following consensus for high-order nonlinear multiagent systems via dynamic output feedback control," *IEEE Trans. Cybern.*, to be published. doi: 10.1109/TCYB.2018.2813423.

[17] E. Garcia, Y. Cao, and D. W. Casbeer, "Periodic event-triggered synchronization of linear multi-agent systems with communication delays," *IEEE Trans. Autom. Control*, vol. 62, no. 1, pp. 366–371, Jan. 2017.

[18] X. Ge, F. Yang, and Q.-L. Han, "Distributed networked control systems: A brief overview," *Inf. Sci.*, vol. 380, pp. 117–131, Feb. 2017.

[19] L. Ding, Q.-L. Han, X. Ge, and X.-M. Zhang, "An overview of recent advances in event-triggered consensus of multiagent systems," *IEEE Trans. Cybern.*, vol. 48, no. 4, pp. 1110–1123, Apr. 2018.

[20] X.-M. Zhang, Q.-L. Han, and X. Yu, "Survey on recent advances in networked control systems," *IEEE Trans. Ind. Inf.*, vol. 12, no. 5, pp. 1740–1752, Oct. 2016.

[21] J. Zhang and G. Feng, "Event-driven observer-based output feedback control for linear systems," *Automatica*, vol. 50, no. 7, pp. 1852–1859, 2014.

[22] H. Li, Z. Chen, L. Wu, H.-K. Lam, and H. Du, "Event-triggered fault detection of nonlinear networked systems," *IEEE Trans. Cybern.*, vol. 47, no. 4, pp. 1041–1052, Apr. 2017.

[23] X. Ge and Q.-L. Han, "Distributed formation control of networked multi-agent systems using a dynamic event-triggered communication mechanism," *IEEE Trans. Ind. Electron.*, vol. 64, no. 10, pp. 8118–8127, Oct. 2017.

[24] D. Yue, E. Tian, and Q.-L. Han, "A delay system method for designing event-triggered controllers of networked control systems," *IEEE Trans. Autom. Control*, vol. 58, no. 2, pp. 475–481, Feb. 2013.

[25] X.-M. Zhang, Q.-L. Han, and B.-L. Zhang, "An overview and deep investigation on sampled-data-based event-triggered control and filtering for networked systems," *IEEE Trans. Ind. Inf.*, vol. 13, no. 1, pp. 4–16, Feb. 2017.

[26] W. P. M. H. Heemels, M. C. F. Donkers, and A. R. Teel, "Periodic event-triggered control for linear systems," *IEEE Trans. Autom. Control*, vol. 58, no. 4, pp. 847–861, Apr. 2013.

[27] H. S. Foroush and S. Martinez, "On triggering control of single-input linear systems under pulse-width modulated dos signals," *SIAM J. Control Optim.*, vol. 54, no. 6, pp. 3084–3105, 2016.

[28] C. D. Persis and P. Tesi, "Input-to-state stabilizing control under denial-of-service," *IEEE Trans. Autom. Control*, vol. 60, no. 11, pp. 2930–2944, Nov. 2015.

[29] A. Cetinkaya, H. Ishii, and T. Hayakawa, "Networked control under random and malicious packet losses," *IEEE Trans. Autom. Control*, vol. 62, no. 5, pp. 2434–2449, May 2017.

[30] S. Feng and P. Tesi, "Resilient control under denial-of-service: Robust design," *Automatica*, vol. 79, pp. 42–51, May 2017.

[31] Y. Zhao, X. He, and D. Zhou, "Optimal joint control and triggering strategies against denial of service attacks: A zero-sum game," *IET Control Theory Appl.*, vol. 11, no. 14, pp. 2352–2360, 2017.

[32] C. Peng, J. Li, and M. R. Fei, "Resilient event-triggering H_∞ load frequency control for multi-area power systems with energy-limited DoS attacks," *IEEE Trans. Power Syst.*, vol. 32, no. 5, pp. 4110–4118, Sep. 2017.

[33] C. D. Persis and P. Tesi, "Networked control of nonlinear systems under denial-of-service," *Syst. Control Lett.*, vol. 96, pp. 124–131, Oct. 2016.

[34] J. Liu, L. Wei, X. Xie, E. G. Tian, and S. Fei, "Quantized stabilization for T–S fuzzy systems with hybrid-triggered mechanism and stochastic cyber-attacks," *IEEE Trans. Fuzzy Syst.*, vol. 26, no. 6, pp. 3820–3834, Dec. 2018.

[35] S. Feng, P. Tesi, and C. De Persis, "Towards stabilization of distributed systems under denial-of-service," in *Proc. 56th IEEE Conf. Decis. Control*, Melbourne, VIC, Australia, 2017, pp. 5360–5365.

[36] X. Ge and Q.-L. Han, "Consensus of multiagent systems subject to partially accessible and overlapping Markovian network topologies," *IEEE Trans. Cybern.*, vol. 47, no. 8, pp. 1807–1819, Aug. 2017.

[37] C. D. Persis and P. Tesi, "Resilient control under denial-of-service," *Proc. IFAC Vol.*, vol. 47, no. 3, pp. 134–139, 2014.

[38] W. H. Chen, J. Zhong, and W. X. Zheng, "Delay-independent stabilization of a class of time-delay systems via periodically intermittent control," *Automatica*, vol. 71, pp. 89–97, Sep. 2016.

[39] W.-A. Zhang and L. Yu, "Stabilization of sampled-data control systems with control inputs missing," *IEEE Trans. Autom. Control*, vol. 55, no. 2, pp. 447–452, Feb. 2010.

[40] L. Schenato, "To zero or to hold control inputs with lossy links?" *IEEE Trans. Autom. Control*, vol. 54, no. 5, pp. 1093–1099, May 2009.

[41] A. Cetinkaya, H. Ishii, and T. Hayakawa, "Event-triggered output feedback control resilient against jamming attacks and random packet losses," *IFAC PapersOnLine*, vol. 48, no. 22, pp. 270–275, 2015.

[42] B.-L. Zhang, Q.-L. Han, and X.-M. Zhang, "Event-triggered H_∞ reliable control for offshore structures in network environments," *J. Sound Vib.*, vol. 368, pp. 1–21, Apr. 2016.

[43] Y.-J. Liu and S. Tong, "Adaptive fuzzy control for a class of nonlinear discrete-time systems with backlash," *IEEE Trans. Fuzzy Syst.*, vol. 22, no. 5, pp. 1359–1365, Oct. 2014.

[44] S. Hu, D. Yue, X. Chen, Z. Cheng, and X. Xie, "Resilient H_∞ filtering for event-triggered networked systems under nonperiodic DoS jamming attacks," *IEEE Trans. Syst., Man, Cybern., Syst.*, to be published. doi: 10.1109/TSMC.2019.2896249.

[45] Y. Li and S. Tong, "Adaptive fuzzy output-feedback stabilization control for a class of switched nonstrict-feedback nonlinear systems," *IEEE Trans. Cybern.*, vol. 47, no. 4, pp. 1007–1016, Apr. 2017.

[46] A. Seuret and F. Gouaisbaut, "Wirtinger-based integral inequality: Application to time-delay systems," *Automatica*, vol. 49, no. 9, pp. 2860–2866, 2013.

[47] X.-M. Zhang, Q.-L. Han, A. Seuret, and F. Gouaisbaut, "An improved reciprocally convex inequality and an augmented Lyapunov–Krasovskii functional for stability of linear systems with time-varying delay," *Automatica*, vol. 84, pp. 221–226, Oct. 2017.

[48] C. Peng, S. Ma, and X. Xie, "Observer-based non-PDC control for networked T–S fuzzy systems with an event-triggered communication," *IEEE Trans. Cybern.*, vol. 47, no. 8, pp. 2279–2287, Aug. 2017.

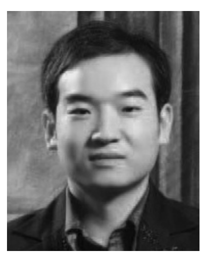

Songlin Hu received the Ph.D. degree in control science and engineering from the Huazhong University of Science and Technology, Wuhan, China, in 2012.

In 2013, he was with the College of Automation, Nanjing University of Posts and Telecommunications, Nanjing, China, where he is currently an Associate Professor with the Institute of Advanced Technology. His current research interests include networked/event-triggered control, T–S fuzzy systems, and time-delay systems.

Dong Yue (SM'08) received the Ph.D. degree in control science and engineering from the South China University of Technology, Guangzhou, China, in 1995.

He is currently a Changjiang Professor and the Dean of the Institute of Advanced Technology, Nanjing University of Posts and Telecommunications, Nanjing, China. His current research interests include analysis and synthesis of networked control systems, multiagent systems, optimal control of power systems, and Internet of Things.

Dr. Yue is currently an Associate Editor of the IEEE TRANSACTIONS ON INDUSTRIAL INFORMATICS, the IEEE TRANSACTIONS ON NEURAL NETWORKS AND LEARNING SYSTEMS, the *Journal of the Franklin Institute*, the *International Journal of Systems Science*, and the IEEE Control Systems Society Conference Editorial Board.

Qing-Long Han (M'09–SM'13–F'19) received the B.Sc. degree in mathematics from Shandong Normal University, Jinan, China, in 1983, and the M.Sc. and Ph.D. degrees in control engineering and electrical engineering from the East China University of Science and Technology, Shanghai, China, in 1992 and 1997, respectively.

From 1997 to 1998, he was a Postdoctoral Researcher Fellow with the Laboratoire d'Automatique etd'Informatique Industielle (currently Laboratoire d'Informatique etd'Automatique pour les Systémes), École Supérieured'Ing'enieurs de Poitiers (currently École NationaleSupérieure d'Ingénieurs de Poitiers), Université de Poitiers, Poitiers, France. From 1999 to 2001, he was a Research Assistant Professor with the Department of Mechanical and Industrial Engineering, Southern Illinois University at Edwardsville, Edwardsville, IL, USA. From 2001 to 2014, he was a Laureate Professor, an Associate Dean of Research and Innovation with the Higher Education Division, and the Founding Director of the Centre for Intelligent and Networked Systems, Central Queensland University, Rockhampton, QLD, Australia. From 2014 to 2016, he was a Deputy Dean of Research with the Griffith Sciences and a Professor with the Griffith School of Engineering, Griffith University, Brisbane, QLD, Australia. In 2016, he joined the Swinburne University of Technology, Melbourne, VIC, Australia, where he is currently the Pro-Vice-Chancellor of Research Quality and a Distinguished Professor. In 2010, he was appointed as a Chang Jiang (Yangtze River) Scholar Chair Professor by the Ministry of Education, Beijing, China. His current research interests include networked control systems, multiagent systems, time-delay systems, complex dynamical systems, and neural networks.

Prof. Han was a recipient of one of the World's Most Influential Scientific Minds: 2014–2016 and 2018, and Highly Cited Researcher Award according to Clarivate Analytics (formerly, Thomson Reuters). He is an Associate Editor of several international journals, including the IEEE TRANSACTIONS ON CYBERNETICS, the IEEE TRANSACTIONS ON INDUSTRIAL ELECTRONICS, the IEEE TRANSACTIONS ON INDUSTRIAL INFORMATICS, the *IEEE Industrial Electronics Magazine*, the IEEE/CAA JOURNAL OF AUTOMATICA SINCA, *Control Engineering Practice*, and *Information Sciences*. He is a fellow of the Institution of Engineers Australia.

Xiangpeng Xie received the B.S. and Ph.D. degrees in engineering from Northeastern University, Shenyang, China, in 2004 and 2010, respectively.

From 2012 to 2014, he was a Postdoctoral Fellow with the Department of Control Science and Engineering, Huazhong University of Science and Technology, Wuhan, China. He is currently an Associate Professor with the Institute of Advanced Technology, Nanjing University of Posts and Telecommunications, Nanjing, China. His current research interests include fuzzy modeling and control synthesis, state estimation, optimization in process industries, and intelligent optimization algorithms.

Xiaoli Chen received the B.Sc. degree in applied mathematics from Xiangfan University, Xiangyang, China, in 2005. She is currently pursuing the Ph.D. degree in telecommunications and information engineering with the Nanjing University of Posts and Telecommunications, Nanjing, China.

Her current research interests include analysis and synthesis of networked control systems, fuzzy systems, interconnected systems, and power systems.

Chunxia Dou received the B.S. and M.S. degrees in automation from Northeast Heavy Machinery Institute, Qiqihar, China, in 1989 and 1994, respectively, and the Ph.D. degree from the Institute of Electrical Engineering, Yanshan University, Qinhuangdao, China, in 2005.

In 2010, she joined the Department of Engineering, Peking University, Beijing, China, where she was a Postdoctoral Fellow for two years. Since 2005, she has been a Professor with the Institute of Electrical Engineering, Yanshan University. She is currently a Professor with the Institute of Advanced Technology, Nanjing University of Posts and Telecommunications, Nanjing, China. Her current research interests include multiagent-based control, event-triggered hybrid control, distributed coordinated control, and multimode switching control and their applications in power systems, microgrids, and smart grids.